Universidade de Lisboa

Faculdade de Ciências

Departamento de Química e Bioquímica

Molecular switches in CFTR processing and trafficking: the role of the novel interactor Rap1A

João Miguel Parente Fernandes

Dissertação

Mestrado em Bioquímica

Especialização em Bioquímica

Orientador: Professor Doutor Carlos Farinha

2011/2012

Index

Acknowledgements

I would like to express my gratitude first and foremost to my supervisor, Prof. Carlos Farinha, who was always very supportive of my work, especially when it didn't go as planned. I owe to him what has become my personal motto in everything concerning life in the lab: try better, fail better. I am also grateful to Prof. Margarida Amaral, for welcoming me into her group and providing me with a very stimulating work environment in which I never lacked for intellectual challenge.

Special thanks are due to the many people in the group which helped me in the daily life in the lab. Sara was a huge support for the whole year, and kept me company everytime I went for snacks or needed to complain (which was very often); this year would have been much duller without her. Simão was always there to point the way in everything biochemical, to provide me with cheesy music and to pester me about my plans for the future. Verónica was always a constant source of laughter and support, especially when we made fun of Sara. I probably wouldn't be presenting this thesis if it weren't for Marisa and her help with the Ussing chambers, with planning experiments, and analyzing data. Thank you for helping me see that I actually had some results! ☺ Marta was as instrumental for my work as everyone else combined, for making all the operations in the lab run smoothly, for providing me with reagents, materials and cells whenever needed and for all the moments of fun. I also had a lot of help from Inna and Anabela, especially with the molecular biology stuff and with the more confusing and unexpected results. Finally, my days in the lab (and out of it) were made a lot more fun by the comraderie and support of Ana Luísa, Ana Margarida, Jorge, Georgina and Johnny Johnny, and lately also by Sara Afonso and Johnny Johnny Johnny.

I am also grateful to Marta Sousa Silva, who was always helpful and interested; I might still be struggling with my cloning experiments if it weren't for the ligase and ligase buffer she kindly provided me.

Outside of the lab, my friends were indispensable. Special thanks are due to Carapeta, for being the perfect wingman, my personal jiminy cricket and an awesome friend. Carlos is an alternating source of fun and boredom, but I would have it no other way, even though he sometimes seems to doubt our friendship. Cátia has long been the most constant of friends and, even though we fight over so many little things, I know she'll be there when I'm in a nursing home, polishing my Nobel Prize in my wheelchair with my hearing aid turned off. To Ruca (born João Tiago Vieira), I hope you know that the fact that I get green with envy every time you talk of your results, or how your thesis

is going, is actually the best compliment I could give you and not a sign of ill will towards you. And I'm sorry I keep forgetting your birthday! ☺

I must also thank my family for supporting me in this five-year endeavor of getting a college education. To my parents; it's been a rocky road, but I think we're getting in the right track. Achieving this was only possible thanks to you and your dedication to my education. To my grandparents, Rita and Eduardo, who gave me an example to follow, a home and wise advice (that I should follow more often), a very big thank you. Finally, I thank my sister (and, sadly, no longer roommate), Damiana, for the camaraderie, support and hours of laughter and to my aunt, Clara, for always being there whenever needed.

I Resumo

A Fibrose Quística é a doença recessiva autossómica letal mais comum na população caucasiana. É caracterizada do ponto de vista clínico por um declínio rápido na função pulmonar, com obstrução das vias aéreas devido à ineficaz remoção de muco e consequentes infecções bacterianas recorrentes. Estas alterações estão associadas desde muito precocemente a um ambiente de hiperinflamação, que exacerba os processos de remodelação do tecido pulmonar e acaba por culminar na fibrose dos tecidos e perda da sua função. Além deste fenótipo respiratório, os pacientes apresentam ainda problemas digestivos graves, nomeadamente a nível pancreático, intestinal e hepático, e são inférteis no caso dos homens e de uma elevada percentagem das mulheres.

A fibrose quística é causada por mutações no gene *CFTR* (do inglês *Cystic Fibrosis Transmembrane Conductance Regulator*) que codifica para uma proteína com o mesmo nome. Neste momento, conhecem-se cerca de 1930 mutações causadoras da doença, sendo a mais comum a delecção de três nucleótidos que correspondem ao resíduo de fenilalanina na posição 508 da proteína. Esta mutação está presente em cerca de 90% dos pacientes.

Esta proteína é expressa em células epiteliais de vários tecidos, e além de funcionar como um canal de cloreto e outros aniões na membrana apical dessas células, é também responsável por regular outros canais e transportadores, tendo um impacto global no transporte iónico epitelial. A fosforilação pela proteína cinase A em resposta a aumento dos níveis de AMP cíclico é considerada o principal mecanismo responsável pela abertura do canal.

Ao ser sintetizada, a CFTR é inserida co-traducionalmente na membrana do retículo endoplasmático, onde adquire a sua conformação nativa com o auxílio de vários chaperones aí presentes e sofre uma glicosilação inicial. Do retículo endoplasmático, é transportada para o Golgi, onde os seus resíduos glicídicos são processados até atingir uma forma madura, que é transportada em vesículas para a membrana plasmática, onde exerce a sua função. Uma vez na membrana, a CFTR é endocitada e segue uma de duas vias: ou é reciclada de volta para a membrana ou é enviada para degradação no lisossoma. O balanço destes processos determina a quantidade de proteína presente na membrana, e como tal são relevantes para a compreensão do defeito molecular que origina a doença..

As interacções que a CFTR estabelece com outras proteínas ao longo deste trajecto são determinantes para que a proteína consiga exercer convenientemente a sua função. Recentemente, a pequena GTPase Rap1A foi identificada como

potencialmente interagindo com a CFTR. O objectivo deste trabalho consistiu na validação dessa interacção e no estabelecimento de um sistema experimental que permitisse avaliar o impacto da Rap1A na biogénese, tráfego e função da CFTR.

A Rap1A é uma pequena GTPase da família Ras que está activa quando ligada a GTP e inactiva quando ligada a GDP. A interconversão destas duas formas é auxiliada por proteínas reguladoras chamadas GEFs (activadores) e GAPs (inactivadores), que respondem a uma variedade de estímulos intra e extracelulares. Quando activa, a Rap1A induz alterações conformacionais em determinadas proteínas alvo, envolvidas na regulação da adesão à matriz extracelular e célula-célula, dinâmica do citoesqueleto e polarização celular, alterando a sua função.

O primeiro passo do trabalho foi avaliar a expressão da Rap1A no tecido mais relevante do ponto de vista clínico, o pulmão. Para isto, realizaram-se experiências de *Western Blot* a partir de culturas primárias de células epiteliais dos brônquios de indíviduos saudáveis e de uma linha celular do epitélio brônquico de pacientes com fibrose quística (CFBE) que sobreexpressa CFTR. Observou-se em ambos os tipos celulares expressão da proteína.

A estratégia escolhida para validar a interacção entre a CFTR e a Rap1A foi tentar co-imunoprecipitar ambas as proteínas. No entanto, não foi possível validar esta associação, tendo sido unicamente observada uma possível colocalização por ensaios de imunofluorescência.

De seguida, foram produzidos com sucesso plasmídeos para expressão da Rap1A *wt* em fusão com GFP, bem como de um mutante constitutivamente activo e um dominante negativo. O protocolo de transfecção de células CFBE com estes plasmídeos e com siRNAs foi optimizado, embora as eficiências de transfecção atingidas tenham sido modestas. A expressão dos constructos fluorescentes foi analisada por *Western Blot* e revelou um problema de *folding* e/ou processamento, provavelmente decorrente da fusão com a GFP. A actividade dos constructos com Rap1A foi também avaliada com um ensaio de actividade específico. Observou-se que o mutante dominante negativo apresentava uma actividade igual ou superior à do constructo *wt*, enquanto o constitutivamente activo apresentava uma actividade igual ou inferior, o que levou a abandonar ambos estes mutantes. Estas discrepâncias em relação à literatura devem-se provavelmente à marcação com GFP. Em nenhuma destas experiências se observaram alterações na quantidade de CFTR total ou madura. O facto de não se ter observado um efeito pode ter sido devido à baixa eficiência de transfecção obtida, à baixa quantidade de proteína com o *folding*/processamento correctos ou devido a uma ausência de efeito.

Finalmente, recorreu-se a câmaras de Ussing para analisar a função da CFTR em monocamadas polarizadas de células CFBE transfectadas com siRNA contra a Rap1A ou siRNA *scrambled*. Não se observaram diferenças na corrente transepitelial induzida pelo tratamento com forscolina (um composto que faz aumentar os níveis de AMP cíclico na célula, activando a CFTR) ou com genisteína (um potenciador específico da CFTR que maximiza a abertura do canal) em células tratadas com siRNA contra a Rap e tratadas com siRNA *scrambled*. Posteriormente, analisando por *Western Blot* a expressão de Rap1A nestas células, concluiu-se que a transfecção foi pouco eficiente, o que justifica a ausência de efeito.

De uma forma geral, houve dois factores limitantes neste trabalho: o facto de, apesar de um longo processo de optimização, as eficiências de transfecção continuarem bastante modestas, e o facto de o sistema de expressão utilizado ser de difícil utilização.

As observações mais significativas resultantes deste trabalho são:

- Tanto em culturas primárias de células epiteliais humanas dos brônquios e em células CFBE41o- observa-se expressão endógena de Rap1A e Epac.

- O padrão de expressão dos factores Epac em células CFBE altera-se quando as células são polarizadas.

- Rap1A é expressa abundantemente nas junções célula-célula no epitélio respiratório, onde co-localiza com a E-caderina.

- A Rap1A parece co-localizar com a CFTR em células do epitélio respiratório polarizadas.

- A quantidade total de CFTR e a quantidade da forma madura (banda C) estão positivamente correlacionadas com os níveis de expressão endógena de Rap1A.

II Abstract

CFTR, the protein whose malfunction causes cystic fibrosis, is a chloride channel expressed in the apical membrane of epithelial cells. CFTR undergoes a long journey in the cell, since it is translated in association with the endoplasmic reticulum until its degradation, throughout which it interacts with numerous proteins. One of these was recently identified as Rap1A, a small GTPase that regulates cell-cell and cell-matrix adhesion, cell polarity and cytoskeleton dynamics. The aim of this work was to validate the interaction between CFTR and Rap1A and evaluate the impact of this small GTPase on CFTR biogenesis, trafficking and function.

Rap1A expression was observed by Western blot in primary cultures of human bronchial epithelial cells and in the CFBE cell line. Plasmids encoding for several variants of GFP-tagged Rap1A were generated. Transfection with these or with siRNAs was optimized, although only sub-optimal efficiencies were achieved. Expression of Rap1A constructs was analysed by Western Blot, revealing a folding and/or processing defect for most constructs. Rap1A activity assays showed that the constitutively active mutant didn't have higher activation levels than the wt construct, whereas the dominant negative had more activity than the wt construct, suggesting that the GFP-tagged constructs were not the most appropriate for this kind of study. No effects on CFTR were observed with Rap1A upregulation, possibly because of the low transfection efficiencies.

Finally, CFTR function upon knockdown of Rap1A was analyzed in Ussing chambers. However, only a minor trend of decrease of CFTR function was observed for Rap1A siRNA transfected samples.

Although suggestive of the need of a different experimental system, the results evidenced that:

- Lung epithelial cells have endogenous expression of Rap1A.

- The band pattern for Epac changed when CFBE cells were polarized;

- Rap1A appears to be enriched in cell-cell junctions, where it co-localizes with E-cadherin;

- Rap1A and CFTR seem to overlap;

- There seems to be a positive correlation between Rap1A levels and both total CFTR expression and band C intensities.

III Abbreviations

ABC – ATP-binding cassete
AF6 – afadin
AKAP – A-kinase anchoring proteins
ARAP3 – ArfGAP with RhoGAP domain, ankyrin repeat and PH domain 3
ATP – adenosine triphosphate
BHK – baby hamster kidney (cell line)
BSA – bovine serum albumin
C3G – CRK SH3-binding GEF
CA – constitutively active
CAAX – cystein-alyphatic-alyphatic-any aminoacid motif
CaCC – calcium activated chloride channel
Calu-3 – human caucasian lung adenocarcinoma (cell line)
cAMP – cyclic adenosine monophosphate
CAPRI – Ca(2+)-promoted Ras inactivator
CCM1/KRI –T-1 cavernous cerebral malformation protein 1/KREV interaction-trapped 1
CF – cystic fibrosis
CFBE41o-/CFBE – cystic fibrosis bronchial epithelial (cell line)
CFTR – cystic fibrosis transmembrane conductance regulator
CHO – chinese hamster ovary (cell line)
CIP – CFTR interacting protein
COP-II – coating protein II
COS-7 – CV-1 (simian) in Origin, and carrying the SV40 genetic material (cell line)
Crk – CT10 Regulator of Kinase
DAPI – 4',6-diamidino-2-phenylindole
DEP – disheveled, Egl-10, pleckstrin domain
dsDNA – double stranded DNA
DMSO – dimethylsulfoxide
DN – dominant negative
E6TP1 – E6-targeted protein 1
E-cad – epithelial cadherin
EDEM – ER degradation-enhancing α-mannosidase-like protein
ENaC – epithelial sodium channel
Epac/Repac – exchange factors directly activated by cAMP
ER – endoplasmic reticulum
ERAD – endoplasmic reticulum-associated degradation
ERM – ezrin-radixin-moesin
ERQC – endoplasmic reticulum quality control
FRET – Förster resonance energy transfer
GAP – GTPase activating protein
GDP – guanosine diphosphate
GEF – guanine nucleotide exchange factor
GFP – green fluorescent protein
GRASP – golgi reassembly stacking protein
GST – glutathione S-transferase
GTP – guanosine triphosphate
GTPase – guanosine triphosphate hydrolase

HBE – human bronchial epithelial cells
Hsc70/Hdj2 – heat shock cognate 70kDa protein/human DnaJ homolog 2
Hsp70/Hdj-1 – heat shock protein with 70kDa/human DnaJ homolog 2
Hsp90 – heat shock protein with 90kDa
HUVEC – human umbilical vein endothelial cells (cell line)
IPTG – Isopropyl β-D-1-thiogalactopyranoside
LB – Luria broth
LKB1 – liver kinase B1
MALDI-TOF – matrix-assisted laser desorption ionization-time of flight
MAPK – mitogen-activated protein kinase
MCF-7 – Michigan Cancer Foundation-7 (cell line)
MDCK – Marbin-Darby canine kidney (cell line)
MEM – minimal essential medium
MS – mass spectrometry
MSD – membrane-spanning domain
NBD – nucleotide binding domain
NHERF – Na+/H+ exchanger regulatory cofactor
ORCC – outwardly rectifying chloride channel
p130-Cas – Crk-associated antigen 130kDa protein
PAGE – poliacrylamide gel electrophoresis
PBS – phosphate buffered saline
PBS-T – phosphate buffered saline supplemented with 0.1% Tween
PCR – polimerase chain reaction
PDZ – post synaptic density protein (PSD95), Drosophila disc large tumor suppressor (Dlg1), and zonula occludens-1 protein (zo-1) domain
PKA – protein kinase A
PVDF – polivinylidene difluoride
qRT-PCR – quantitative real-time polimerase chain reaction
R-domain – regulatory domain
RA-RhoGAP – Rap-activated Rho GTPase-activating protein
RAPL – Rap ligand
RASAL – Ras GTPase-activating-like protein
RBD – Rap-binding domain
RIAM – Rap1-GTP-interacting adaptor molecule
ROMK – renal outer medullary potassium channel
RT – room temperature
siRNA – small interfering RNA
SDS – sodium dodecylsulphate
SNARE –soluble N-ethyl-maleimide sensitive factor Attachment Protein receptors
Spa-1 – signal-induced proliferation-associated gene-1
SPAL – Spa-1-like protein
SPAR – surfactant protein A binding protein
TIAM1 – T-lymphoma invasion and metastasis-inducing protein 1
UGGT – UDP-glycoprotein glucosyltransferase
UPS – unfolded protein response
VASP – Vasodilator-stimulated phosphoprotein
VE-cad – vascular endothelium cadherin
YFP – yellow fluorescent protein

1 Introduction

1.1 Cystic Fibrosis - Overview

Cystic Fibrosis (CF) is the most common lethal autosomic recessive disorder in the Caucasian population. It affects 1 in 2500 to 6000 live births and has a carrier frequency of 1 in 25 to 40 individuals. The disease frequency is variable among different ethnic groups, being highest in Northeastern Europe and quite rare among Oriental populations (1:90,000)[1].

It was first described in 1938 as a disorder of its own right by Anderson and colleagues, who also came to find that it had a recessive autossomal pattern of inheritance. At the time of its discovery as a disease in its own right, cystic fibrosis was described as a digestive disorder, since the first detectable symptoms were intestinal obstruction in newborns and malnutrition in infants, and was associated with a progressive fibrosis of the pancreatic tissue. Because infants died at a very young age, these were the only symptoms that were noticeable. As the digestive problems in newborns and children were gradually overcome with the advances in healthcare, problems in the respiratory tract became the major cause for morbidity and mortality.

In 1953, an excess of salt in the sweat of patients was identified, which was later attributed to a defect in chloride transport in the sweat glands. This defective chloride transport was also detected in the lung, pancreas and intestinal epithelium, the most affected tissues[1]. In 1989, the gene responsible for the disease was identified using a positional cloning strategy and cautiously named cystic fibrosis transmembrane conductance regulator (CFTR). This gene encodes for a cAMP-regulated chloride channel expressed in a number of epithelial tissues. It was found to harbour mutations in all CF patients analysed, the most common of which being a deletion of three nucleotides encoding for a phenylalanine in position 508 in the protein (ΔF508, or F508del as it is most commonly termed now)[2]. This mutation is present in about 90% of all patients, and represents only one of the 1930 mutations in the CF gene described at the time this work was written[3].

Even though CF research has gone a long way since then, therapies targeting the molecular basis are only now starting to appear and reach the patients. This has only been possible thanks to international, concerted effort in understanding the molecular mechanisms governing CFTR biogenesis and function in health and disease, which will be discussed in this Introduction.

1.2 Clinical features of Cystic Fibrosis and therapeutics

Clinical features of CF are dominated by involvement of the respiratory tract, with obstruction of the airways by thick, dehydrated airway mucus that prevents proper mucocilliary clearance. This leads to recurring bacterial infections, especially with *Pseudomonas aeruginosa* and *Staphylococcus aureus* species. A hyperinflammation environment is generated in the lungs of patients from a very early age, exacerbating tissue remodelling processes and fibrosis[4]. This degradation of the lung tissue and loss of its function is the main cause of morbidity and mortality among CF patients. The involvement of the gastrointestinal tract is also common, with 85% of the patients presenting pancreatic insufficiency as a result of the obstruction of the pancreatic ducts. 10 to 20% of newborns with CF present a form of intestinal obstruction called *meconium ileus*, and 2 to 5% develop liver disease at some time during the course of the disease. In adults with CF, infertility is almost universal in males, due to congenital bilateral absence of the vas deferens, and is also frequent in females. Patients also have elevated concentrations of sodium chloride in the sweat; in fact, the sweat test, which measures the amount of salt in the sweat of patients, is still one of the fundamental tools for the establishment of a CF diagnosis[5].

Because there are so many different disease-causing mutations in CFTR, mutation-specific treatments are not a viable option. Therefore, they have been grouped in classes based on the functional defect they confer, in order to facilitate the establishment of common therapeutic strategies. Class I mutations abolish protein production. Class II mutations result in defective protein processing; this is the case of the most common F508del mutation. Class III proteins confer defects in the regulation of the channel. Class IV mutations have a defective ion conductance. Class V mutations result in decreased protein synthesis. Class VI mutations decrease the protein's stability in the membrane.

Most of the different therapeutic approaches that have been used in the last 25 years focus mainly on the amelioration of the symptoms of CF. This includes anti-inflammatory and antibiotic drugs, as well as treatments directed towards restoring the levels of airway surface liquid, preventing mucus accumulation and overcoming the nutritional defects in patients. Currently, therapeutic focused research includes a multiplicity of approaches: search of candidate modifier proteins to identify new potential therapeutic targets and pharmacological therapy to rescue the molecular defects responsible for CF are the most important topics under development[6]. In January 2012, Kalydeco, the first drug targeting the molecular basis of the disease, was approved by the Food and Drugs Administration in the USA. This compound,

previously named VX-770, corrects the gating defect conferred by several mutations, and has been approved for patients over 6 years of age with the G551D mutation. Clynical phenotype of patients with the much more common F508del mutation is significantly improved by this drug; aditionally, ongoing clinical trials are exploring a combination of VX-770 with another compound, VX-809, that corrects the trafficking defect of proteins with other mutations, including F508del[7].

1.3 CFTR structure

The CFTR gene (or ABCC7), is one of the longest in the human genome, approximately 250kb long, and encompasses 27 exons in total. It generates transcripts of about 6.5kb after splicing, which are translated into a protein with 1480 aminoacid residues.

This protein was identified soon after its discovery as a member of the ATP-binding cassette (ABC) transporter family due to structure similarity. Like other ABC transporters, it has two membrane spanning domains (MSDs) with six transmembrane segments each, portions of which form the pore through which anions pass, and two nucleotide binding domains (NBD1 and NBD2). Both NBDs bind and hydrolyse ATP, which drives channel opening and closure, respectively. Recent experimental data suggest that this is linked to dimerization of these two domains[8]. The most common mutation in cystic fibrosis patients, F508del, is located in the NBD1. In the structure of CFTR there is also a regulatory (R) domain that is absent in all other ABC transporters which contains consensus sites for phosphorylation by various kinases, including protein kinase A (PKA). Phosphorylation of the R domain by PKA in response to cyclic AMP is regarded as the major determinant for opening of the channel. In the C-terminus, CFTR has a PSD95, Dlg1, ZO-1 (PDZ)-binding motif through which it is involved in complex PDZ-based protein interaction networks with a number of proteins[9]. The N-terminus is also a site for interaction with other proteins, as will be discussed in section 1.7.

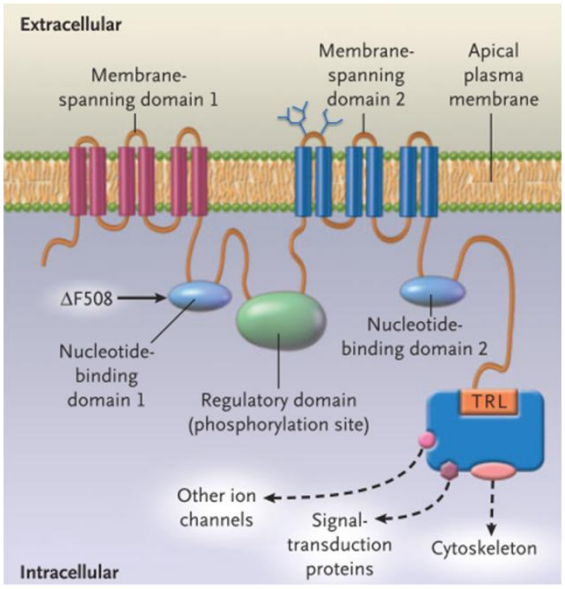

Figure 1.1 - Schematic representation of the structure of CFTR. Taken from Rowe (2005)[5].

1.4 CFTR function

The traditional function attributed to CFTR is that of a chloride channel. Contrary to other ABC transporters, CFTR is incapable of actively driving ion transport against a gradient; instead, it functions as a passive channel that allows bidirectional flow of ions when open.

The gating of the CFTR Cl^- channel is tightly controlled by the balance of kinase and phosphatase activity in the cell and by cellular ATP levels. Activation of PKA by cAMP causes phosphorylation of multiple serine residues within the R domain. Once the R domain is phosphorylated, channel gating is regulated by a cycle of ATP hydrolysis at the NBDs. Finally, protein phosphatases dephosphorylate the R domain and return the channel to its quiescent state[10].

This PKA-mediated activation of CFTR depends on the strict compartmentalization of cAMP in the cell. It has been shown that the increase in cAMP necessary for PKA to activate CFTR must be specifically localized near the membrane, in the subcortical compartment[11]. This compartmentalization is dependent on the integrity of the subcortical cytoskeleton and on the presence of A-kinase anchoring proteins (AKAPs), such as Na^+/H^+ exchange regulatory co-factors (NHERFs) and ezrin, which anchor PKA, phosphatases, phosphodiesterases and other signaling proteins near CFTR and close to the membrane[12].

CFTR function is not restricted to being a chloride channel, though. It also permeates other anions, namely bicarbonate and glutathione.

It is still debated to what extent CFTR, and not the Cl^-/HCO_3^- transporter, which is also expressed in most secretory epithelia, is responsible for bicarbonate transport *in vivo*, because its permeability to this ion is low (only about 25% of that of chloride). However, the fact is that bicarbonate transport is impaired in CF patients, and this accounts at least partially for the loss of pancreatic function[13,14], so even if it doesn't directly permeate this anion it probably regulates channels/transporters that are involved in the process.

Glutathione transport by CFTR, on the other hand, is a well established fact, and it has important effects on the extracellular redox balance, mucocilliary clearance, inflammation and immune response, processes that are impaired in the CF airways and pancreas. Defects in extracellular glutathione homeostasis have been proposed to be one of the major contributors to the exacerbation of inflammation and consequent deterioration of the lung tissue in CF[15,16].

Besides acting as an ion channel itself, CFTR also regulates other channels in the cell membrane. The mechanisms underlying this are hard to pin down, because it is not easy to distinguish between effects caused by changes in CFTR itself from those that are consequences of altered chloride conductance. Regulation of the epithelial sodium channel (ENaC) by CFTR is the most studied of these phenomena. ENaC is inhibited by increased CFTR activity, even in chloride-free media. There are three main possible causes for this: an increased chloride conductance might have effects *per se* in ENaC; CFTR and ENaC might be part of a macromolecular complex with proteins that regulate ENaC by themselves; or CFTR and ENaC might interact directly with one another. Compelling evidence exists to support any of these three hypotheses, so no consensus has been reached so far in this matter. CFTR also regulates other ion channels, including outwardly rectifying chloride channels (ORCCs), renal outer medullary potassium channel (ROMK)[17], and calcium activated chloride channels (CaCCs)[18].

1.5 CFTR folding

Because CFTR is such a large membrane protein, proper folding is difficult to achieve. In fact, at least in heterologous expression systems, depending on the cell type, only 20-40% of the protein escapes the endoplasmic reticulum quality control (ERQC) system and reaches its native conformation, with the rest being tagged for degradation by the ubiquitin-proteasome pathway. Whereas the NBD1 folds mostly co-translationally, the native structure of the NBD2, and therefore of the full channel, is

only attained post-translationally. This slow, stepwise folding is facilitated by the interaction with several chaperones at the endoplasmic reticulum (ER)[19].

As CFTR begins to be translated by the ribosome, an ER targeting motif is recognized by the signal recognition particle, causing it to be taken to the surface of the ER and co-translationally inserted in the ER membrane via the translocon complex. While the nascent polypeptide chain is being inserted in the ER membrane, the exposed parts in the cytosol associate with the cytosolic molecular chaperones Hsp90, Hsc70/Hdj-2, and Hsp70/Hdj-1. A branched 14-unit oligosaccharide is added at asparagine residues 894 and 900 in the fourth extracellular loop in a process called N-glycosylation or core-glycosylation[20]. Initially, this glycosidic moiety has three glucose residues that are trimmed away by glucosidases I and II. The chaperones calnexin and calreticulin recognize the monoglucosylated intermediate and shield it from the highly crowded environment of the ER, preventing unwanted interactions and aggregation with other molecules and allowing folding to progress. The protein then dissociates from calnexin/calreticulin and has its last glucose residue removed.

If the protein is folded at this point, it proceeds to the secretory pathway. If, however, the protein didn't attain the proper folding, it is recognized by UDP-glycoprotein glucosyltransferase (UGGT), which re-glucosylates it and begins the next round of chaperone binding, deglucosylation and proofreading. If the protein undergoes too many of these rounds, eventually it becomes subject to ER-associated degradation (ERAD): it is marked by the ER degradation-enhancing α-mannosidase-like protein (EDEM) for degradation, is retrotranslocated to the cytoplasm and degraded by the ubiquitin-proteasome pathway.

Most of the CFTR bearing the F508del mutation falls victim to the ERQC system and is degraded before evading the ER into the Golgi[21].

1.6 CFTR trafficking

If CFTR folds properly and is allowed to progress to the secretory pathway, it is loaded into COP II-coated vesicles that bud from the ER and traffic to the Golgi. Along the Golgi, its glycosidic moiety is further processed into a mature, fully glycosylated, transport-competent form. This form has a lower electrophoretic mobility than the core-glycosylated protein, allowing their easy distinction by Western Blotting as band C and band B, respectively. After this fine processing, CFTR is incorporated into secretory vesicles that deliver the protein into the apical membrane, where it will exert its functions[22]. Alternatively, some data suggests that at least a portion of CFTR may be

delivered directly from the ER to the apical membrane without going through the Golgi through a GRASP-dependent pathway[23].

Not surprisingly, CFTR trafficking to the membrane in epithelial cells is dependent on their polarization state[24]. Cell polarization is characterized by, among other things, a selective redistribution of membrane proteins among the apical and basolateral sides, which relies on polarized sorting and trafficking of those proteins[25]. However, the precise molecular mechanisms governing polarization-dependent delivery of CFTR to the apical membrane have not been well studied.

After being delivered to the membrane, CFTR becomes subject to endocytosis. CFTR is internalized into early endosomes, where it can either be targeted to recycling vesicles containing Rab11, which will be returned to the apical membrane, or sent to the lysosome for degradation[26].

All these processes depend on the loading, budding, docking and fusing machinery that regulate intracellular trafficking that comprise a huge number of proteins, including Rab GTPases and soluble NSF Attachment Protein receptors (SNAREs).

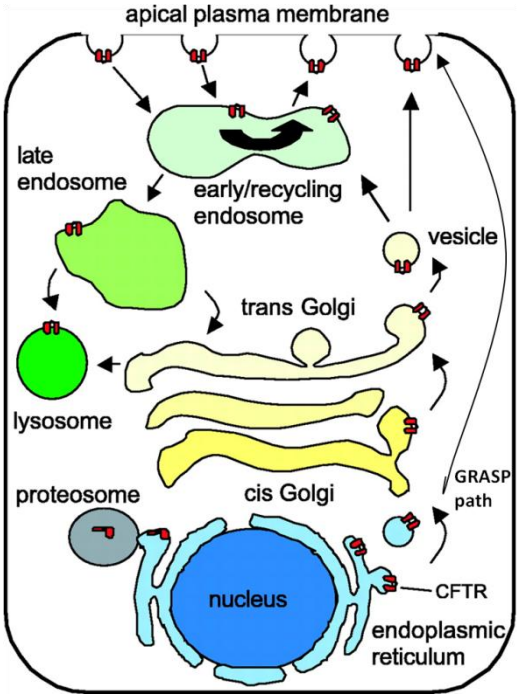

Figure 1.2 - Schematic representation of CFTR trafficking, starting at the endoplasmic reticulum. Adapted from Bertrand (2003)[27].

1.7 The CFTR interactome and Rap1A

Throughout its lifetime, CFTR makes a very long travel in the cell, that begins with translation in the cytoplasm, traversing the ER and Golgi to the membrane, and being

recycled or sent for degradation. Along this journey, CFTR interacts with numerous proteins that have all sorts of effects on it. Throughout the previous sections of this Introduction, a reasonably large number of proteins have been mentioned as being relevant in CFTR biogenesis, from kinases, scaffolding proteins and chaperones to trafficking small GTPases and SNAREs. The number of known CFTR-interacting proteins (CIPs) is staggering, and it keeps on growing. Understanding how CFTR interacts with all these partners and how they affect it is crucial for proper therapeutic strategies to be devised that target the molecular basis of cystic fibrosis.

Proteomic technologies are especially well suited to identify CIPs[28,29]. In 2010, Faria and other colleagues from our group reported having identified several CIPs with one such approach[30]. Using a recombinant CFTR NBD1 as affinity chromatography bait, CIPs in Calu3 (a human airway epithelial cell line) cell extracts were captured, separated by 2D gel electrophoresis and identified by MALDI-TOF. One of the proteins identified was a small GTPase called Rap1A, which will be described in the following sections.

1.8 Rap1A – an overview

Rap1A is a small GTPase belonging to the Ras superfamily of GTPases, specifically to the Rap subfamily. It was discovered in the late 1980s for its ability to revert the morphological phenotype of Ras-transformed cells. It was initially postulated that it merely competed for binding to Ras effectors without activating them, but this view has been challenged with the appearance of a myriad of Rap modulators and interactors with varying specificities. Rap1A is seen nowadays as a node in a complex signaling pathway of its own, which interacts with several other signaling pathways involved in key biological processes in the cell. The most prominent of these is control of cell adhesion, both to the extracellular matrix and to neighboring cells. It also takes part in regulating actin cytoskeleton dynamics and cell polarity (both in resting states and during cell migration), exocytosis and membrane protein recycling, and it might have a role in cell cycle regulation[31].

There are 5 known members of the Rap family: Rap1A and B and Rap2A, B and C. Rap2 proteins are mainly expressed in platelets and other hematopoietic cells, whereas Rap1A and B are expressed in a broader range of human tissues, including the lung, colon and pancreas, the most affected tissues in cystic fibrosis. Rap1A, on which this work is focused, is 181 residues long and approximately 21kDa when mature.

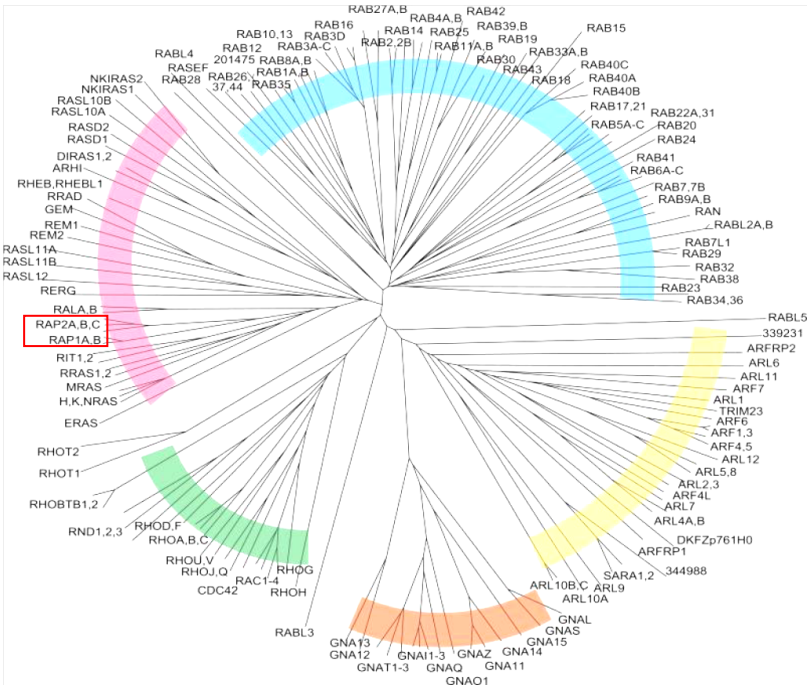

Figure 1.3 - The Ras superfamily of GTPases, with the Rap subfamily outlined in red. Adapted from Colicelli (2004)[32].

Rap1A, like all other small GTPases, cycles between two structural conformations. When it binds GTP, Rap1A is in an active form, capable of binding to and inducing specific conformational changes in downstream effectors. When it binds GDP it shifts to an inactive form, which is incapable of interacting with those effectors. The intrinsic GTPasic activity and nucleotide release rate of Rap1A are very low, so when it binds GTP it tends to stay locked in the active conformation, and when it binds GDP it remains in the inactive conformation, thus functioning as a molecular switch. Interconversion of these two conformations depends on auxiliary regulatory proteins that either activate or inactivate Rap1A. Activators are called guanine nucleotide exchange factors (GEFs) and act by stimulating the release of the bound GDP, allowing for binding of the much more abundant GTP. GTPase activating proteins (GAPs), on the other hand, are actually Rap inactivators, because when they increase the very low GTPase activity of the protein, which is where their designation comes from, they lead to hydrolysis of the bound GTP to GDP, converting Rap1A in the inactive form. Several GEFs and GAPs with varying specificities for Rap1A have been identified and characterized, and will be adressed in section 1.10.

The localization of Rap1A is essential to its function, as it must be close to both its activators and downstream effectors in order to have an effect in the cell. Rap1A localization is defined by its post-translational modifications, which are discussed in section 1.9. While some other GTPases, from the Rho family, for instance, translocate

between the cytosol and the membrane (depending whether they bind proteins that mask the lipid anchor or not), the localization of Rap proteins doesn't vary a lot. Instead, Rap signaling is spatially and temporally controlled by regulating the localization and activation state of RapGEFs and GAPs, respectively, as will be discussed in section 1.10.

1.9 Rap1A post-translational modifications

Rap1A is subject to four kinds of posttranslational modifications necessary for its proper function: prenylation and methylation of Cys181, proteolysis of the 3 C-terminal residues and phosphorylation of Ser180. Rap1A contains a CAAX (C – cysteine, A – any aliphatic aminoacid, X – any aminoacid) consensus motif in the very end of the C-terminus that is recognized by geranylgeranyl transferase 1. The Cys residue is geranylgeranylated, the three last residues are proteolitically removed by a CAAX protease and the cysteine, now the last residue in the C-terminus, is methylated by a methyl transferase. The X residue at the C-terminus determines what kind of lipid anchor is added to the protein; for instance, Rap1A, Rap1B and Rap2A all end with leucine and are geranylgeranylated, whereas as Rap2B, which ends with glutamine, is farnesylated[33]. Experimental information concerning Rap2C prenylation has not been obtained so far. Phosphorylation of Rap1A by PKA at Ser180 appears to have an effect on its function, affecting its ability to bind some downstream effectors[34].

Due to its geranylgeranyl anchor, Rap1A localizes to membranes in the cell. It has been reported to be either perinuclear and co-localized with Golgi markers in COS-7[35] cells or in a late endocytic vesicular compartment in the fibroblast cell lines BHK, NIH3T3[36] and C2[37]. In endothelial cells, namely HUVECs[38], and in epithelial cells, such as MCF-7[39] and MDCK[40] cells, Rap1A is seen at the plasma membrane and enriched at cell-cell junction sites. Two papers reported that in CHO[41], which are epithelial-like, and A549[42] cells, which are epithelial, Rap1A has been identified in perinuclear locations; however, in these reports, cells were cultured in suspension, which may explain why Rap1A was located differently than in other epithelial cell lines. It seems to be a general rule that in endothelial and epithelial cells, when grown in conditions that allow for cell-cell adhesion to develop, Rap1A is located at cell junctions.

Prenylation seems to be necessary for the membrane localization of Rap1A, but it doesn't seem to affect which membranes it localizes to. Instead, an internal TAQST sequence between residues 85 and 89 seems to be responsible for its perinuclear location in COS-7 cells. It is unclear how it functions in maintaining Rap1A at the nuclear periphery in fibroblasts but not in endothelial and epithelial cells. It is likely that

this differential behavior involves interaction with other proteins differentially expressed in these distinct cell types, but this doesn't seem to have been explored so far[35].

1.10 RapGEFs and RapGAPs

Rap GEFs are much better understood than GAPs, and great effort has been focused on understanding how they activate Rap in a spatially and temporally strict way. Most of them respond to extracellular stimuli, relayed by either second messengers or tyrosine kinase receptors. Many of them also activate other Ras-family GTPases to lesser extents[43].

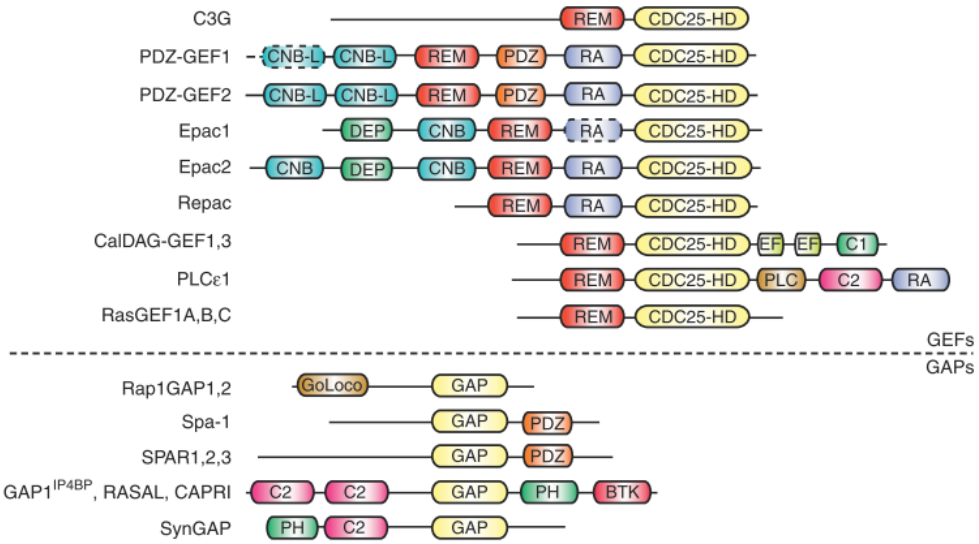

Figure 1.4 - Schematic representation of the multi-domain structure of RapGEFs and RapGAPs. Taken from Gloerich (2011)[44].

Epac is a 104kDa multidomain protein that activates Rap proteins in response to direct binding of cAMP, constituting a cAMP sensor in the cell that is independent of protein kinase A (PKA). Binding to cAMP has a double action on Epac: it activates it, allowing it to activate Rap in its turn, and it induces its translocation to the plasma membrane. The disheveled, Egl-10, pleckstrin domain (DEP) is necessary for this translocation and has been shown to tether Epac to phosphatydic acid in the membrane.

Epac is also tethered to the plasma membrane by phosphorylated (active) ezrin, radixin and moesin (ERM) scaffolding proteins. It is worthy of note that ezrin also interacts with CFTR (through E3KARP/NHERF2) and with PKA, forming a macromolecular complex that facilitates phosphorylation of CFTR and its activation[12]. Ezrin also tethers CFTR to the actin cytoskeleton, increasing its membrane stability[11]. Radixin has also been reported to bind Epac and PKA simultaneously, bringing these two cAMP sensors together[45]. All these data suggest that Epac might co-localize with

CFTR, which argues for a possible function of Rap1A in regulating CFTR function or membrane stability. Besides, Epac is activated by stimuli that result in increased subcortical cAMP, the same stimuli that induce PKA-mediated activation of CFTR, which further supports this hypothesis.

C3G is another GEF that has been shown to mediate signals received from B and T cell receptor activation, growth factors, cytokines, G protein coupled receptors and integrins. C3G is present in the cytoplasm in a complex with members of the Crk family of small adapter molecules. In response to stimuli, this complex is recruited to the cell membrane. This involves association of Crk with phosphotyrosine containing proteins like receptor tyrosine kinases, p130 Cas, insulin receptor substrate 1 and paxillin. Phosphorylation of C3G by Src-family kinases is also important in this translocation from cytosol to cell membrane. At the membrane, C3G activates downstream signaling by Rap1, Rap2 and R-Ras.

Other GEFs include PDZ-GEFs, which are involved in cadherin-mediated cell-adhesion and polarization and localize active Rap1 to the cortical cytoskeleton near the plasma membrane, and CalDAG-GEFs, which activate Rap1 upon binding to diacylglycerol, another important second messenger.

Rap GAPs include RapGAPs I and II, the SPA-1 family (SPA-1, SPAR, SPAL, and E6TP1), and tuberin. These are specific to Rap proteins, but even though the catalytic mechanisms for Rap and Ras deactivation are different, some GAPs exist that have dual activity, namely GAP1^{IP4BP}, GAP1^{m}, CAPRI, and RASAL[46]. Most research on these regulators has focused on catalytic mechanisms and on the role of RapGAPs in tumorigenesis rather than in elucidating how they regulate Rap signaling.

1.11 Rap effectors and function

Rap signaling has been implicated in a growing number of cellular processes, of which the most prominent is cell adhesion, both between cells and between the cell and the extracellular matrix. The involvement of Rap in the establishment of cell polarity will also be discussed. Its role in cell migration, cell cycle regulation, lymphocyte-specific (reactive oxygen species formation, B- and T-cell receptor signaling) and neuron-specific functions (neurite outgrowth, synaptic plasticity) are beyond the scope of this work.

All these functions are implicit in the set of proteins whose activity or localization Rap modulates. By interacting with VASP (an actin polymerizing protein)[47], the RhoGEFs TIAM, Vav2[48] and FRG[49] and the RhoGAPs ARAP3[50] and RA-RhoGAP[51], Rap signaling causes sometimes drastic changes in cytoskeleton dynamics. Interaction

with Afadin/AF6 and p120-catenin is necessary for the regulation of E-cadherin stability at nascent adherens junctions in epithelial cells[52], and interaction with CCM1/KRIT provides a similar role in VE-cadherin-based adherens junctions in the endothelium[53]. By activating the effectors RAPL and RIAM, Rap proteins are involved in the activation and clustering of various integrins and consequently in adhesion to several extracellular matrix proteins, including fibronectin, fibrinogen, collagen and laminin[31]. Adhesion to the extracellular matrix doesn't seem to affect Rap signaling, though, so this phenomenon seems to be unilateral. Depending on the cell type and mode of activation, Rap1 can also activate B-Raf, a serine/threonine kinase that regulates the MAPK signaling pathway[54].

The regulation of cadherin stability at adherens junction by Rap signaling is one of the subjects of major focus in Rap-related research. Stabilization of newly-recruited E-cadherin in nascent adherens junctions is dependent on Rap1 and is mediated by p120-catenin[52].Although, as stated above (see section 1.9), Rap1 in epithelial cells is located mainly at the plasma membrane, upon the loss of adherens junctions it translocates to recycling vesicles that also contain endocytosed E-cadherin and Rab11. Furthermore, disengagement of adherens junctions results in activation of Rap1 via C3G, which facilitates E-cadherin recycling to the membrane and allows adherens junctions to be reformed[40]. It is interesting to note that recycling of CFTR also involves sorting to Rab11-positive vesicles[26], making this a possible meeting point between both proteins.

Rap proteins have a well described role in the establishment of cell polarity in neurons, where they define which out of a number of seemingly equal dendrites becomes the axon. In yeasts, budding is also spatially controlled in a similar fashion[55]. However, information is still scarce in what concerns the role of Rap signaling in the establishment of epithelial cell polarity. It has been shown that it is necessary for Arg kinase-dependent polarization in 3D cultures of MDCK cells[56]. It is also known that, in hepatocytes, the bile acid taurocholate increases cAMP levels in the cytoplasm, which are relayed to Rap1 by Epac and eventually result in the activation of the kinase LKB1, a master regulator of polarization in many cell types[54]. Although a role for LKB1 in the polarization of lung epithelial cells has only been shown so far in adenocarcinomas, it is plausible to think that this signaling module might be relevant for polarization of these cells in normal conditions as well. Whether this is the case or not, an effect of Rap1 in polarization can have an impact on CFTR biogenesis, as the delivery of CFTR to the membrane is dependent on proper cell polarization.

2 Objectives

The global aims of this work were to validate the previously reported interaction between Rap1A and CFTR and to assess the impact of up- and down-regulation of this small GTPase on CFTR biogenesis. In order to achieve this, several milestones were established, namely:

1 – To validate the interaction between Rap1A and CFTR through co-immunoprecipitation and immunofluorescence;

2 – To produce plasmid constructs suitable for expression of GFP-tagged wt, constitutively active and dominant negative Rap1A;

3 – To optimize transfection conditions with plasmids and siRNA and assess Rap1A expression and activity in transfected cells;

4 – To evaluate the effect of up- and down-regulation of Rap1A on CFTR expression, trafficking and function.

3 Materials and Methods

3.1 Production and characterization of vectors to study the impact of Rap1A on CFTR biogenesis

3.1.1 Bacterial strain

The bacterial strain used for cloning and DNA amplification was XL1-Blue (Stratagene, La Jolla, CA, USA), which is tetracycline resistant. XL1-Blue cells are endonuclease (endA) deficient, which greatly improves the quality of miniprep DNA, and are recombination (recA) deficient, improving insert stability. The hsdR mutation prevents the cleavage of cloned DNA by the EcoK endonuclease system. The lacIqZ Δ M15 gene on the F´ episome allows blue-white color screening.

XL1-Blue Genotype: recA1 endA1 gyrA96 thi-1 hsdR17 supE44 relA1 lac [F´ proAB lacIqZ Δ M15 Tn10 (Tetr)]. (Genes listed signify mutant alleles. Genes on the F´ episome, however, are wild-type unless indicated otherwise).

3.1.2 Plasmid vectors and siRNAs

pCMV6-AC-Rap1A-GFP (RG215248, Origene, Rockvile, MD, US), which encodes for a Rap1A-GFP fusion protein (GFP tag at the C-terminus of Rap1A), and pCMV6-AN-GFP (PS100048, Origene), a destination vector for expression of proteins with a GFP tag in the N-terminus, were used. Maps and cloning schemes for both vectors are available in Appendices 1 and 2. Both plasmids contain the ampicillin resistance gene, which was used for selection of transformed bacteria.

The fragment containing the Rap1A open reading frame was cloned from pCMV6-AC-Rap1A-GFP into pCMV6-AN-GFP, yielding the pCMV6-AN-GFP-Rap1A plasmid, as described in section 3.1.7. Variants of pCMV6-AN-GFP-Rap1A encoding for constitutively active (G12V) and dominant negative (S17A) mutants of Rap1A were obtained by site-directed mutagenesis, as described in section 3.1.8.

siRNAs used were Silencer Select Negative control #2 (4390846), Rap1A siRNA (s11781) and CFTR siRNA (52945) (all from Applied Biosystems, Foster City, CA, USA).

3.1.3 Production of competent bacteria

Bacteria were plated in LB-agar medium supplemented with tetracycline and a single colony was used to inoculate a small volume of LB medium overnight at 37°C with vigorous shaking (220 rpm). This pre-inoculum was then used to inoculate at dilution 1/100 a larger volume of LB medium, typically 100 ml, which was also grown at

37°C (220 rpm) to final concentration of 5 x 10^7 bacteria/ml (corresponding to an absorbance of 0.3 at 600 nm). Bacteria were transferred to ice and pelleted by centrifugation (1000 g for 15 min at 4°C). The bacterial pellet was then ressuspended, incubated on ice for 15 min in 33mL RF1 buffer (100 mM RbCl, 50mM $MnCl_2$, 30 mM KCH_3COO pH 7.5, 10 mM $CaCl_2$, 15% (w/v) glycerol, pH 5.8; all from Sigma-Aldrich, St. Louis, MO, USA) and re-pelleted by centrifugation (1000 g for 15 min at 4°C). This second pellet was ressuspended and incubated on ice for 15 min in 8.3mL RF2 buffer (10 mM MOPS, 10mM RbCl, 75mM $CaCl_2$, 15% (w/v) glycerol, pH 6.8; all from Sigma-Aldrich). 200 µl aliquots were then rapidly frozen with liquid nitrogen and stored at -80°C.

3.1.4 Transformation of competent bacteria

Bacteria were transformed by incubating a 200 µl aliquot of competent cells with DNA (100-200ng of ligation products; 0.1-10ng of plasmid DNA) for 30 min on ice, followed by heat-shock (2min at 42°C), incubation for 3min on ice, and then allowing antibiotic resistance to be expressed by growth in antibiotic-free LB medium for 45 min at 37°C at 220rpm. Bacteria were then pelleted (5000g for 2min), the supernatant was discarded and the pellet was ressuspended in the remaining supernatant medium. This suspension was then plated into LB-agar supplemented with selection antibiotic (100 µg/ml ampicillin, Sigma-Aldrich) and left to grow overnight.

Transformed bacterial colonies were grown in LB medium supplemented with 100µg/mL ampicillin and used to extract plasmid DNA. Clones were stored in liquid LB medium supplemented with 15 % (w/v) glycerol (Sigma-Aldrich) at -20°C.

3.1.5 DNA extraction and quantification

Small scale plasmid DNA was purified with the PeqGOLD Plasmid Miniprep Kit (PeqLab, Erlangen, Germany). This protocol is based on an alkaline lysis of the bacterial cells in the presence of SDS, to denature bacterial proteins, followed by a centrifugation step to remove cellular debris, genomic DNA and denatured proteins, and adsorption of the plasmid DNA in the supernatant to an anionic exchange matrix in the presence of high saline concentrations. After adsorption, the DNA is washed and eluted in water or TE buffer (10mM Tris/HCl, EDTA 1mM, pH8). Sequence of plasmid DNA preparations was confirmed by automatic DNA sequencing at least once for every plasmid.

DNA concentration was determined by measurement of absorbance at 260nm (one absorbance unit corresponding to 50µg/ml of dsDNA) using a Nanodrop 2000 spectrophotometer (Thermo Scientific, Waltham, MA, USA) and its purity was

evaluated by assessment of the ratio A260/A280. Only DNA with a ratio above 1.8 was considered pure enough for further use.

3.1.6 DNA sequencing

Plasmid DNAs were purified as described in section 3.1.5. The sequencing reactions were performed using the ABI Prism BigDye Terminator Cycle Sequencing Kit (Applied Biosystems) according to the manufacturer's instructions. The products were analyzed in the automatic sequencer 3130 XL Genetic Analyzer (Applied Biosystems). Alternatively, the sequencing reactions were outsourced to StabVida, using BigDye Terminator 3 (Applied Biosystems) and analysed in a ABI 3730XL sequencer (Applied Biosystems). Sequencing primers used were VP1.5 (forward primer, sequence 5'-GGACTTTCCAAAATGTCG-3') and XL39 (reverse primer, sequence 5'-ATTAGGACAAGGCTGGTGGG-3') (obtained through Thermo Scientific).

For sequence analysis, the sequences obtained were analysed through comparison with the reference human *Rap1A* sequence (NCBI reference sequence NM_002884.2) using the software Bioedit (http://www.mbio.ncsu.edu/BioEdit/bioedit.html).

3.1.7 Cloning

The fragment containing the Rap1A open reading frame was cloned from pCMV6-AC-Rap1A-GFP into pCMV6-AN-GFP. Briefly, the two plasmids were separately hydrolysed with MluI and AsiAI (an SgfI isoschizomer) (Fermentas, Burlington, Canada) and the resulting fragments were separated by low-melting agarose gel electrophoresis. The bands containing the fragments of interest were excised from the gel and melted at 70ºC. The melted portions of gel containing insert and empty vector were combined at a ratio of 4:1, respectively, and incubated with ligase and ligase buffer (Roche) for 72h at 4ºC. Bacteria were then transformed with the ligation product, plated in LB-Agar plates supplemented with ampicillin 5ug/mL and allowed to grow overnight at 37ºC. Single colonies were picked to LB medium with ampicillin 5ug/mL and grown for plasmid extraction and sequencing. One clone containing the correct recombinant plasmid, pCMV6-AN-GFP-Rap1A, was chosen for further use.

3.1.8 Mutagenesis

Mutations were introduced into pCMV6-AN-GFP-Rap1A using the KOD Hot Start Kit (Novagene, Darmstadt, Germany) with complementary pairs of the custom designed HPLC-purified mutagenic primers described in Table 3.2 (Thermo Electron Corporation, Waltham, MA, USA). Primers were designed with the software PrimerX (http://www.bioinformatics.org/primerx).

The mutagenesis reaction is a regular PCR reaction, with the peculiarity being that the primers are not completely complementary to the template sequence; instead, they contain the desired point mutations. The PCR programs used are displayed in Table 3.1. The result of this mutagenesis reaction is a mixture of the template plasmid and a new nicked plasmid containing the desired mutations. After confirming the amplification by agarose gel electrophoresis, the PCR products were incubated with *DpnI* (Invitrogen, Carlsbad, CA, USA), a restriction enzyme that specifically hydrolyzes methylated and hemi-methylated DNA. This results in complete degradation of the template DNA, which was produced in bacteria and, thus, is heavily methylated. The mutagenized plasmid, however, was synthesized *in vitro* and was not methylated, therefore resisting to hydrolysis by DpnI.

Table 3.1- PCR programs used for the mutagenesis reactions

	Temperature	Time	Number of cycles
Program used for mutagenesis with DeltaT, TAAins and S17A primers	95ºC	2min	25
	95ºC	20s	
	50ºC	10s	
	72ºC	5min	
Program used for mutagenesis with G12V primers	95ºC	2min	26
	95ºC	20s	
	46.5ºC	11s	
	72ºC	3min30s	

After the hydrolysis step, bacteria were transformed with the PCR products (section 3.1.4 from this Chapter). Bacteria not only amplify the plasmid DNA but also repair the nicks left by the polymerase. Following transformation, plasmid DNA was extracted (section 3.1.5 from this Chapter) and the presence of each mutation was confirmed by automatic DNA sequencing (section 3.1.6 from this Chapter).

Table 3.2 - Primers for mutagenesis reaction. The table presents only the forward primers. For each, a complementary reverse primer was also used.

Name	Sequence
G12V	5'- GGTCCTTGGTTCAGTGGGCGTTGGGAAGTC -3'
G15D	5'- GTTCAGGAGGCGTTGACAAGTCTGCTCTGAC -3'
S17A	5'- GTTCAGGAGGCGTTGGGAAGGCCGCTCTGACAGTTCAGTTTG -3'
DeltaT	5'- GGTGTAACTGTGCCTTTTTAGAATCTTCTGCAAAGTC -3'
TAAins	5'- CATGTCTGCTGCTCTAAACGCGTTAAGCGGC -3'

3.2 Biochemical and electrophysiological analysis of Rap1A impact on CFTR biogenesis

3.2.1 Characterization, Culture and Maintenance of cell lines

The majority of the experiments were performed in CFBE41o- cells[57] (cystic fibrosis bronchial epithelial, further referred to simply as CFBE) stably overexpressing wt CFTR. This cell line is one of the most commonly used cell models for the study of CFTR in a lung context. Because they are able to polarize, these cells mimic what happens in the lung epithelium in physiological conditions.

Cells were cultured in Minimal Essential Medium supplemented with L-alanyl-L-glutamine (MEM+Glutamax) (Gibco, Paisley, UK), 10% (v/v) fetal bovine serum and 100U/mL penicillin and 100mg/mL streptomycin (Invitrogen) in plastic flasks or plates coated with LHC basal medium (Invitrogen), bovine serum albumin, fraction V 0.1mg/mL, collagen from rat tail 29µg/mL and fibronectin 10µg/mL (all from Roche). For polarization-dependent assays, cells were seeded in either Snapwell (Sigma-Aldrich) or Millicell (Millipore, Billerica, MA, USA) filters at a density of $2x10^5$ cells/filter coated with collagen IV (Sigma-Aldrich) and cultured with MEM+Glutamax supplemented with 5% fetal bovine serum (FBS) and 100U/mL penicillin and 100mg/mL streptomycin on both apical and basolateral compartments. Transepithelial resistance was measured every other day with an STX2 Chopstick Electrode (World Precision Instruments, Inc., Sarasota, FL, USA), in order to monitor monolayer integrity, and experiments were performed when it exceeded $750\Omega.cm^2$.

Primary cultures of human bronchial cells (HBE) from 3 healthy donors were prepared by Marta Palma in our unit. The access to explanted lungs was established through a collaborative project between the Faculty of Sciences of the

University of Lisboa and the Cardio-Thoracic Surgery Department of the Hospital de Santa Marta (Lisboa), which received approval from the hospital's Ethics Committee, and primary HBE cells were isolated as described in reference 58.

Continuous growth was made possible by pre-confluence enzymatic dissociation with trypsin (Invitrogen). After dissociation, cells were resuspended and redistributed in new flasks or plates. Cell lines were stored in liquid nitrogen in aliquots in 40% (v/v) Minimal Essential Medium (Gibco), 50 % (v/v) FBS (Invitrogen) and 10 % (v/v) DMSO (Sigma-Aldrich), a cryoprotectant that prevents the formation of ice crystals during the freezing process. Freezing was performed in such a way that the cooling speed was about 1ºC/min, in order to minimize damage to the cells. Thawing was done by quickly submerging the vials in water at RT, washing the cells with F12 Medium (Invitrogen) and seeding in the medium described above.

Cultures were maintained at 37ºC in a humidified atmosphere of 5% (v/v) CO_2.

3.2.2 Transfection

CFBE cells were transfected using either cationic liposomes or electroporation.

Lipofection is based on the ability of cationic lipids to form unilamelar liposomes that adsorb nucleic acid molecules to their surface and are internalized by the cells. The delivery mechanisms of the nucleic acid to the cytoplasm and nucleus are poorly understood, but the practical result is protein expression (plasmids) or down-regulation of the target genes (siRNAs)[59]. In this work, several such liposomal formulations were used, namely Lipofectamine 2000 (Invitrogen), Fugene HD (Promega, Fitchburg, WI, US) and Hiperfect (Qiagen, Venlo, Netherlands). Liposomal solutions and DNA or siRNA were separately incubated for 5 min in OPTIMEM (Invitrogen), mixed together and allowed to incubate for 15 min at room temperature (RT). They were then added dropwise to either 70-80% confluent cells or freshly trypsinized cells. Medium was changed after 24h and the experiments were performed 48-72h post-transfection.

Another way of transfecting cells is by delivering the plasmid DNA or siRNA through an electrical shock. This causes transient, reversible changes in the organization of the lipid bilayer in the membrane, resulting in the opening of pores big enough for nucleic acids to enter[60]. A Microporator MP100 (Digital Bio, Seoul, South Korea) was used for electroporation experiments. Briefly, $1x10^5$ cells were mixed with 1.5μg of the appropriate DNA or siRNA, pipetted into a gold-covered tip and delivered a certain number of electrical pulses. Pulse voltage ranged from 1075-1500V, pulse width from 10 to 25ms and the number of pulses was 2-3. Cells were then seeded in

12-well plates in the medium described in section 3.2.1. Medium was changed after 24h and the experiments were performed 48-72h post-transfection.

For transfection with plasmids, which encode for GFP or GFP fusion proteins, transfection efficiency was estimated by direct counting of fluorescent vs. non fluorescent cells under an epifluorescence microscope (check brand). This was only feasible when the number of attached cells at 24h post-transfection was relatively small. When there was a great number of attached cells, and for siRNAs, transfection efficiency could only be evaluated by Western Blot.

3.2.3 Preparation of total protein extracts

For Western blot (WB), protein extracts were prepared by cell lysis with sample buffer (1.5 % (w/v) SDS; 5 % (v/v) glycerol; 0.01 % (w/v) bromophenol blue; 0.05 mM dithiotreitol; 0.095 M Tris pH 6.8) and DNA was sheared by passing the sample first through a 22G and then a 27G needle until viscosity decreased or sheared by enzymatic action of 5-25U/mL of benzonase (Sigma-Aldrich) in the presence of $MgCl_2$ 2.5mM.

Total protein concentration in different samples was assessed by a modified Lowry protein assay. Proteins were solubilized with 0.015% (w/v) sodium deoxycholate for 10 min at RT, precipitated with 6% (w/v) trichloroacetic acid and then centrifuged at 14000 g for 5 min. The supernatant was removed and the pellet was resuspended in equal volumes of H_2O and Reagent A (0.1 g/l $CuSO_4.5H_20$; 0.2 g/l potassium tartarate; 10 g/l Na_2CO_3; 2.5% (w/v) SDS; 0.2 M NaOH) followed by 10 min incubation at RT. Finally, Reagent B (Folin-Ciocalteau Reagent diluted 5-fold in water) was added, followed by incubation for 30 min. Protein concentration was determined by measurement of A_{750} and comparison with a regression line obtained for BSA (BioRad, Hercules, CA, USA) standards of increasing concentrations.

3.2.4 Western blot

After quantification of total protein (see section 3.2.3), protein extracts were separated by SDS-polyacrylamide gel electrophoresis (PAGE) on 7, 10 or 12.5% (w/v) mini-gels, followed by transfer onto Immobilon polivinylidene difluoride (PVDF) -membranes (Millipore). After blocking with 5 % (w/v) skimmed milk in phosphate-buffered saline (PBS, NaCl 137mM; KCl 2.7mM; KH_2PO_4 1.5mM; Na_2HPO_4 6,5mM, pH 7.4) containing 0.1% (v/v) Tween (PBS-T) for 2 h, the membranes were probed for 2 h at RT with primary antibodies diluted in 5% (w/v) milk in PBS-T, washed 3x10min with PBS-T, followed by incubation for 1 h at RT with horseradish peroxidase-conjugated secondary antibodies in 5% (w/v) milk-PBS-T. Blots were developed either by

autoradiography or using the Chemidoc XRS$^+$ analyser (BioRad). When autoradiographic detection was chosen, the signal was developed using the Immobilon kit (Millipore). Films were digitalized (Sharp JX-330, Amersham Biosciences, Uppsala, Sweden) and integrated peak areas were determined using ImageQuant TL software (GE Healthcare, Uppsala, Sweden). When the Chemidoc XRS$^+$ was used, the signal was developed with the ImmunStar Western C Chemiluminescence kit (BioRad) and quantification was performed with the ImageLab software (BioRad).

3.2.5 Rap1A activity assay

The active fraction of Rap1A was purified using the pull-down assay described in reference [61]. This assay is based in the specific interaction between the Rap-binding domain (RBD) of RalGDS and active, GTP-binding Rap1A. This domain was expressed fused with glutathione S-transferase, which strongly binds to glutathione-coupled agarose beads. These beads are then used to selectively pull-down active Rap1A in cell extracts.

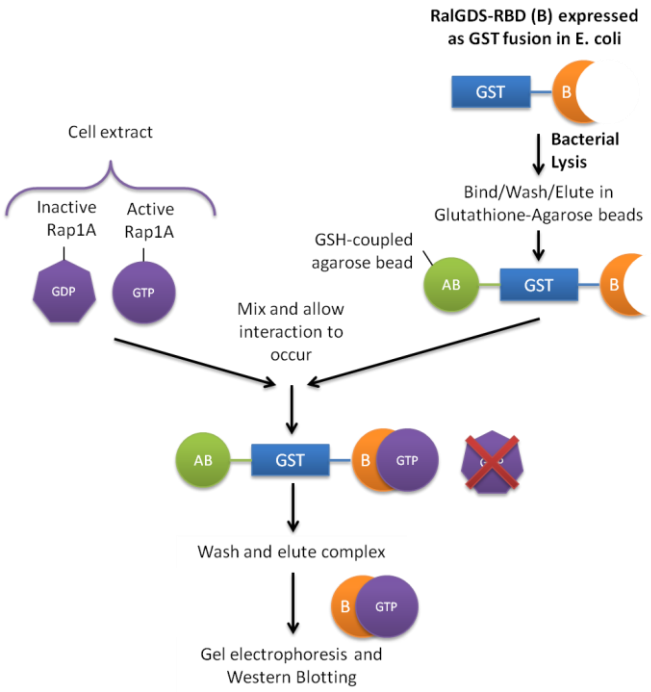

Figure 3.1 - Schematic representation of the Rap1A activity assay.

For the preparation of the beads, bacteria transformed with pGEX-RalGDS-RBD-GST (a kind gift from Dr.David Altschuler, University of Pittsburgh School of Medicine) were grown in LB liquid medium until an OD_{600} of 0.6 was reached at which expression of the RalGDS-RBD-GST fusion protein was induced with IPTG 1mM (NZYTech, Lisbon, Portugal) for 4h. After centrifugation to collect bacteria, these were resuspended in PBS containing 1x Complete protease inhibitor cocktail (Roche, Basel,

Switzerland) and sonicated 10x 10 cycles of 0.7s. Proteins were solubilized with 1% (v/v) Triton X-100 (Pharmacia Biotech, GE Healthcare, Chalfont St. Giles, UK) for 30 min at 4ºC, centrifuged at 10 000 g, 10 min and incubated with glutathione agarose beads (Molecular Probes, Eugene, OR, USA) for 1-2 hours at 4ºC. The beads were then diluted 1:1 in PBS and a 50% slurry was added 1:1 to glycerol and stored and -80ºC.

Induction of expression of the recombinant protein was monitored by running aliquots of the lysates (taken before and after addition of IPTG) in an SDS-PAGE gel, which was stained with Coomassie blue, showing robust expression after adding IPTG. Recombinant protein pull-down was monitored by running aliquots of beads taken before and after incubation with the bacterial lysates in an SDS-PAGE gel and staining with Coomassie blue, confirming that the protein was effectively captured.

For the pull-down assays, cells were lysed on ice in Rap1A lysis buffer (25mM Tris-HCl, 1% (v/v) NP-40, 5mM $MgCl_2$, 150mM NaCl, 0.1mM DTT, 5% (v/v) glycerol, Complete protease inhibitor cocktail, pH 7.5) for 15 min. Lysates were clarified by centrifugation and incubated with glutathione agarose beads coupled to GST-RalGDS for 1 hour at 4ºC. Beads were washed and resuspended in 1x sample buffer for analysis by Western Blot.

3.2.6 Immunoprecipitation

CFBE cells overexpressing wt CFTR were grown in P100 plates until confluency was reached, lysed with 1mL PD buffer (50mM Tris-HCl, 0.1M NaCl, 1% (v/v) NP40 (Roche), 10% (v/v) glycerol, supplemented with a 1x Complete protease inhibitor cocktail, pH 7.5) at 4ºC and collected with a cell scraper. Cell membranes and debris were pelleted by centrifugation at 10000rpm for 5min at 4ºC and the supernatant was incubated at 4 ºC overnight with the appropriate antibody and 40uL of Protein-G agarose beads (25μg) (Invitrogen). The beads were pelleted by centrifugation for 1min at 13000rpms, washed 3x with wash buffer (Tris-HCl 0.1M pH 7.5, NaCl 0.3M, Triton X-100 1% (v/v)) and eluted with 1x sample buffer. The immunoprecipitate was electrophoretically separated on SDS-PAGE gels and analysed by Western Blots (see section 3.2.4).

3.2.7 Immunofluorescence

Cells were grown in filters to achieve polarization (see section 3.2.1) until a minimum resistance of $800\Omega/cm^2$ was reached. Cells were washed 3x with PBS, fixed for 30min-1h with 4% (v/v) formaldehyde, washed 3x with PBS, permeabilized for 10-15min with Triton X-100 0.5% (v/v) and washed again 3x with PBS. A blocking step

with PBS with 1% (w/v) BSA (30min) was performed to avoid unspecific binding of the antibodies. The filter with cells was cut into several pieces with an adequate size for imaging and each piece was incubated in a humid chamber with a specific primary antibody diluted in PBS with BSA 1% (w/v) for 1h. The filter pieces were washed 3x with PBS with Triton X-100 0.05% (v/v) and incubated in a humid chamber with secondary antibody diluted in PBS with BSA 1% (w/v) for 1h. Filters were then washed 3x with PBS with Triton X-100 0.05% (v/v), post-fixed with 4% (v/v) formaldehyde for 10min and washed again 3x with PBS with Triton X-100 0.05% (v/v). The filter pieces were mounted in glass slides with Vectashield mounting medium (Vector Laboratories, Burlingame, CA, USA) containing DAPI (Sigma-Aldrich) and sealed. Immunofluorescence staining was observed in a Zeiss Axiovert 200M microscope (Zeiss, Jena, Germany) orin a Leica DMI4000B confocal microscope (Leica Microsystems, Wetzlar, Germany).

3.2.8 Antibodies

Antibodies used are summarized in Table 3.3.

Table 3.3 - List of primary and secondary antibodies used.

	Antigen	Cat. No. (Brand)	Application (Dilution)
Primary antibodies	CFTR (NBD2)	596 (Cystic Fibrosis Foundation)	WB (1:3000), IP (1:1000)
	CFTR (R domain)	570 (Cystic Fibrosis Foundation)	IF (1:250 for wt, 1:200 for F508del CFTR)
	Rap1A	sc-1482 (Santa Cruz Biotechnology, Santa Cruz, CA, US)	WB (1:200), IF (1:50), IP (1:100)
	α-tubulin	T5168 (Sigma	WB (1:20000-1:30000)
	Epac/RapGEF3	ARP52140_P050 (Aviva Systems Biology, San Diego, CA, US)	WB (1:1000)
	E-cadherin	610181 (BD Biosciences, San Jose, CA, US)	IF (1:200)
	GFP	11814460001 (Roche)	WB (1:1000)
Secondary antibodies	Mouse IgG, HRP-conjugated	NA931V (Amersham)	WB (1:3000)
	Rabbit IgG, HRP-conjugated	NA934VS (Amersham)	WB (1:5000)
	Mouse IgG, Alexa 568-conjugated	A10037 (Invitrogen)	IF (1:500)
	Rabbit IgG, Alexa 488-conjugated	A21206 (Invitrogen)	IF (1:500)

3.2.9 Ussing Chamber assays

Briefly, the basolateral surface of the CFBE monolayers grown in Snapwell (Sigma-Aldrich) filters was continuously perfused (5 ml/min) with Ringer solution of the following composition: NaCl 145mM, KH_2PO_4 0.4mM, K_2HPO_4 1.6mM, D-glucose 5mM, $MgCl_2$ 1mM, calcium gluconate 1.3mM. The apical bath solution was perfused with a

low Cl^- Ringer solution containing: NaCl 32mM; KH_2PO_4 0.4mM; K_2HPO_4 1.6mM; D-glucose 5mM; $MgCl_2$ 1mM; calcium gluconate 5.7mM and sodium gluconate 112mM. The pH of all bath solutions was adjusted to 7.4 and all experiments were carried out at 37 °C under open circuit conditions. Cell monolayers were equilibrated in the micro-Ussing chambers for at least 20min in perfused Ringer solution before the experimental protocol and then perfused sequentially with the cAMP-elevating agent forskolin at 2μM, forskolin 2μM and the CFTR potentiatior genistein at 25μM, and finally with the specific CFTR inhibitor CFTR Inh172 30μM.

Values for the transepithelial voltage (V_{te}) were recorded continuously and were referred to the basolateral surface of the epithelium. Transepithelial resistance (R_{te}) was determined by applying intermittent (1s) current pulses (0.5μA). The equivalent short-circuit current (I_{sc}) was calculated according to Ohm's law ($I_{sc} = V_{te} / R_{te}$)[62,63].

4 Results

4.1 Rap1A expression in CFBE cells and primary cultures of human bronchial cells

The central question of this work, whether or not Rap1A has an impact on CFTR biogenesis, is only relevant if Rap1A is expressed in the same cells where CFTR has an important function. Since the most clinically relevant defect in cystic fibrosis is caused by CFTR malfunction in the lung epithelium, it was of special interest to see if Rap1A was expressed in lung epithelial cells. To answer this question, Rap1A expression was assessed by Western blotting in the CFBE wt cell line and in primary cultures of human bronchial epithelial cells from three healthy donors, using a specific Rap1A antibody. Since the RapGEF Epac is activated by cAMP (the same second messenger that signals for CFTR activation) its expression was also evaluated.

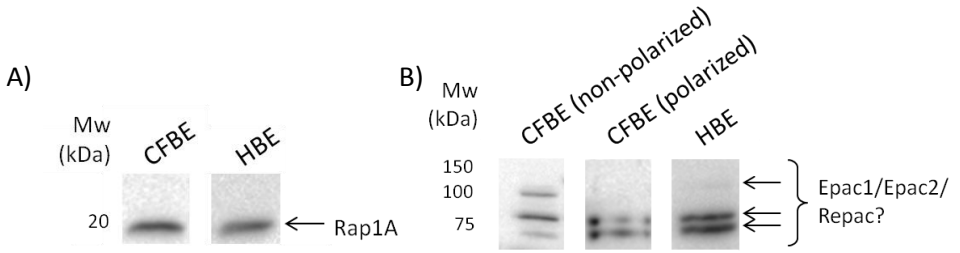

Figure 4.1 - Western blot of protein extracts from CFBE and HBE cells using A) anti-Rap1A antibody and B) anti-Epac1 antibody. HBE cells were always grown in filters and polarized. The HBE blots are representative of experiments with cells from 3 different non-CF donors.

Rap1A expression was confirmed with the appearance of a ~20kDa band in HBE and CFBE cells (both polarized in filters and grown in plastic, with no differences). Later on, this ~20kDa band was seen to disappear in CFBE cells transfected with Rap1A siRNA, confirming its identity (see Figure 4.8).

Regarding Epac expression, it is harder to be sure how to interpret the band pattern obtained. The Epac family comprises 3 members: Epac1 (104kDa), Epac2 (115kDa) and Repac (63kDa). Although it was raised against Epac1, the antibody might be able to detect the other highly homologous Epacs, especially being a polyclonal antibody. Also, Epac1 might be subject to alternative splicing, yielding two different isoforms of 104 and 66kDa (UniprotKB accession numbers O95398 and O95398-2, respectively), further complicating the interpretation of the Western blot. This would need further experiments to clarify: RT-PCR with isoform specific primers to analyse mRNA expression, knockdown with isoform-specific siRNAs to compare the Western blot band patterns or detection by mass spectrometry are some possibilities.

Regardless of this, the bands that were present in the Western blots were clear and had high intensities, suggesting that they are specific, thus indicating that some isoforms of Epac are expressed in these cells. Interestingly, the band pattern for the Epac antibody changed when CFBE cells were polarized, something that hasn't been reported in the literature so far.

With the expression of Rap1A confirmed, its localization was assessed by immunofluorescence in polarized CFBE wt cells, in parallel with staining for CFTR and E-cadherin.

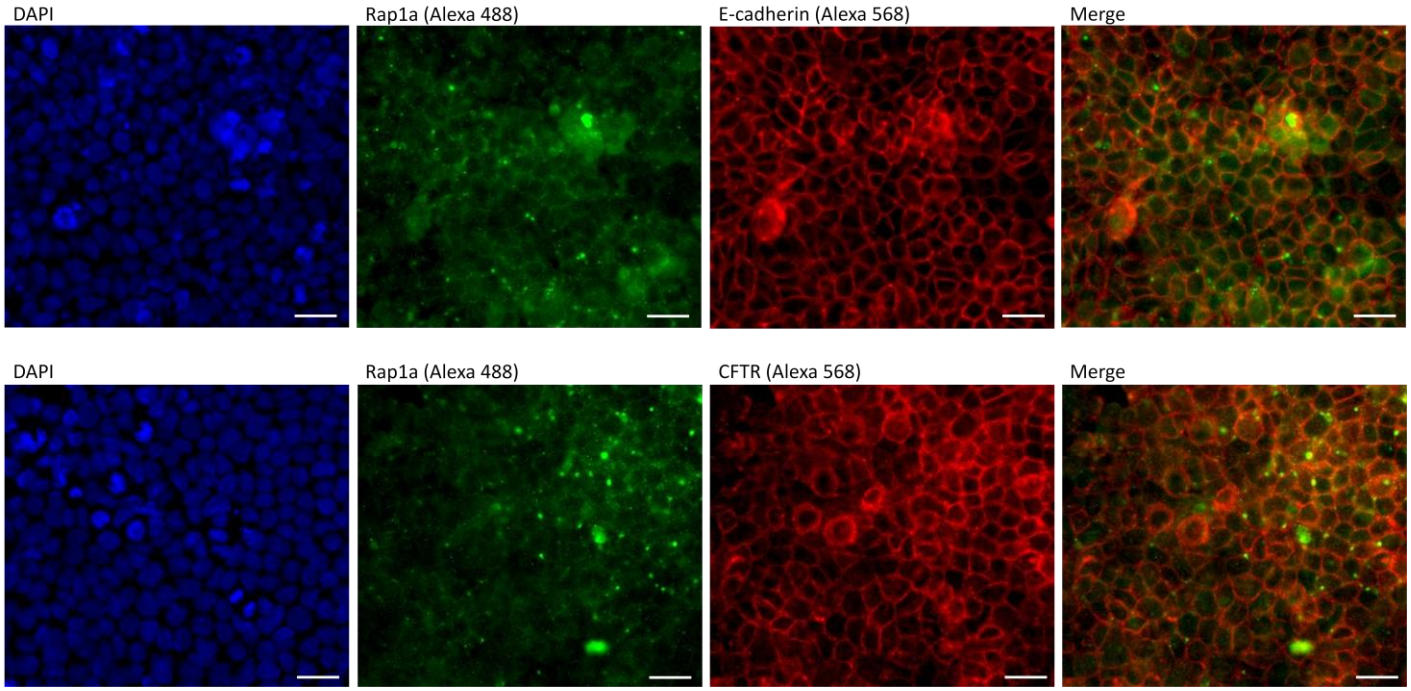

Figure 4.2- Localization of endogenous Rap1A, CFTR and E-cadherin in polarized CFBE wt cells. Scale bar=50µm.

Staining of endogenous Rap1A gave signals of very low intensity, even though the antibody was at a high concentration. The protein seems to have a dispersed localization in the cell, either in the cytoplasm or the plasma membrane. However, it appears to be enriched in cell-cell junctions, where it co-localizes with E-cadherin. This is expected, as Rap1A is reported to be located in adherens junctions in other epithelial cell types, namely in the Marbin-Darby canine kidney (MDCK) cell line[64]. The distribution of Rap1A and CFTR also seem to overlap, which supports a possible interaction, but this is difficult to ascertain due to the weak staining for endogenous Rap1A.

4.2 Co-immunoprecipitation

To evaluate the proposed interaction between Rap1A and CFTR, co-immunoprecipitation experiments were performed.

Overexpressed CFTR and endogenous Rap1A were immunoprecipitated in parallel, and cross-detection in the immunoprecipitates was performed by Western Blotting. A negative control was included in which the whole protocol was done without the addition of antibodies, to discard any non-specific binding to the Protein-G-coupled agarose beads.

Results however were inconclusive, hardly indicating the presence of Rap1A in the same protein complexes as CFTR.

4.3 Molecular cloning and mutagenesis

The next task consisted in producing plasmid vectors for expression of Rap1A, as well as three mutants previously reported in the literature. These mutants were:

- G12V, which is reported to display constitutive activation[65];
- G15D, which is insensitive to Epac but is still capable of being activated by C3G;
- S17A, which has been described as the most effective dominant negative in the literature[66].

The starting materials, which were already available in the lab prior to the start of the work, were pCMV6-AC-Rap1A-GFP, a plasmid which encodes for a wt Rap1A fused with an GFP-tag in its C-terminus, and pCMV6-AN-GFP, an empty vector designed for expression of N-terminally GFP-tagged proteins. pCMV6-AC-Rap1A-GFP has an SgfI restriction site at the beginning of the Rap1A ORF and an MluI site at the end, which are compatible with sites for the same enzymes in the pCMV6-AN-GFP vector. Both vectors also encode for ampicillin and neomycin resistance genes for selection in bacteria and mammalian cells, respectively. Plasmid maps are included in the Appendices (section 0).

First of all, the original plasmids were sequenced. Analysis of the sequences revealed an insertion of one thymine in the middle of the Rap1A ORF, which caused the downstream portion of the ORF to be out of frame. A preliminary mutagenesis reaction was performed to eliminate this problem using the DeltaT primers and program described in section 3.1.8.

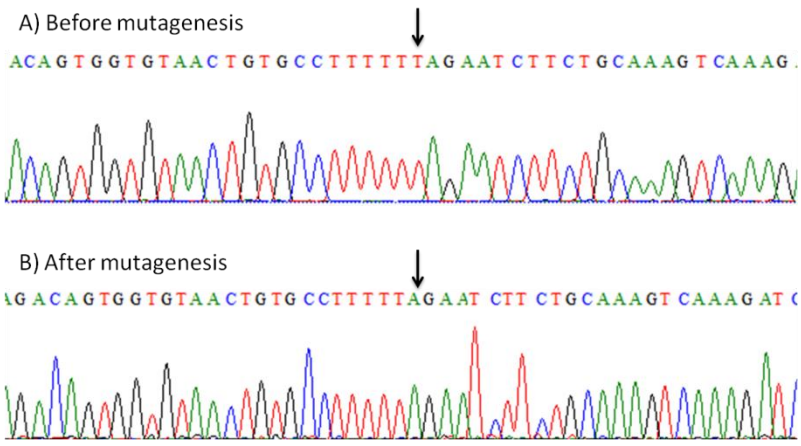

Figure 4.3 - Sequence of the original pCMV6-AC-Rap1A-GFP plasmid showing A) an insertion of a T and B) removal of this T after the mutagenesis.

To circumvent possible folding and stability issues caused by the introduction of the GFP-tag on the C-terminus of the protein, it was found useful to also have a vector for expression of an N-tagged construct. Upon further research into the literature, this was considered an absolute necessity, due to the fact that Rap1A is subject to geranylgeranylation, proteolysis and methylation in the conserved CAAX motif in its C-terminus. A C-terminal GFP tag is likely to mask this recognition site, disrupting the protein's processing, localization and function, as was later seen to be the case. Therefore, the Rap1A cDNA in pCMV6-AC-Rap1A-GFP was cloned into pCMV6-AN-GFP.

The cloning procedure was performed as described in the section 3.1.2 of the Materials and Methods. Ligation products were used to transform bacteria, after which several transformed colonies were picked and grown separately in liquid medium. Plasmids were then purified and four clones were analyzed by agarose gel electrophoresis to confirm insertion of the Rap1A cDNA, which can be seen in Figure 4.4.

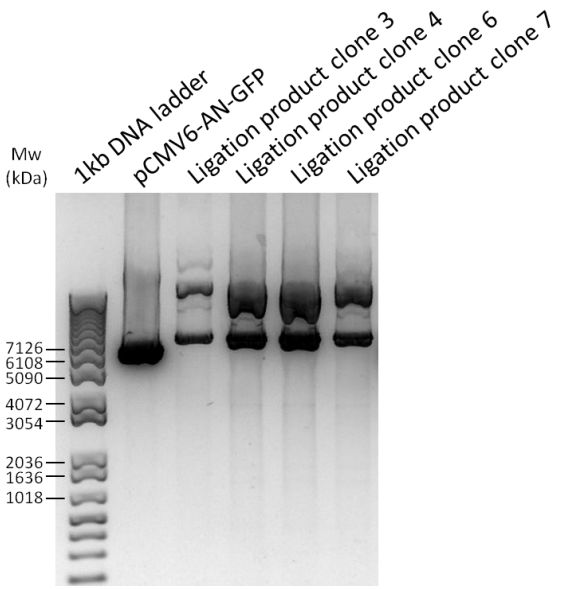

Figure 4.4 - Agarose gel electrophoresis of the products of ligation of the Rap1A cDNA from pCMV6-AC-Rap1A-GFP into the pCMV6-AN-GFP vector.

Plasmids extracted from all four clones showed a decrease in their electrophoretic mobilities, suggesting an increase in mass that was compatible with the insertion of the 555bp Rap1A cDNA.

These plasmids were then sequenced (Section 3.1.6) to confirm successful ligation, as shown in Figure 4.5. A single clone (clone 6) was selected for further use.

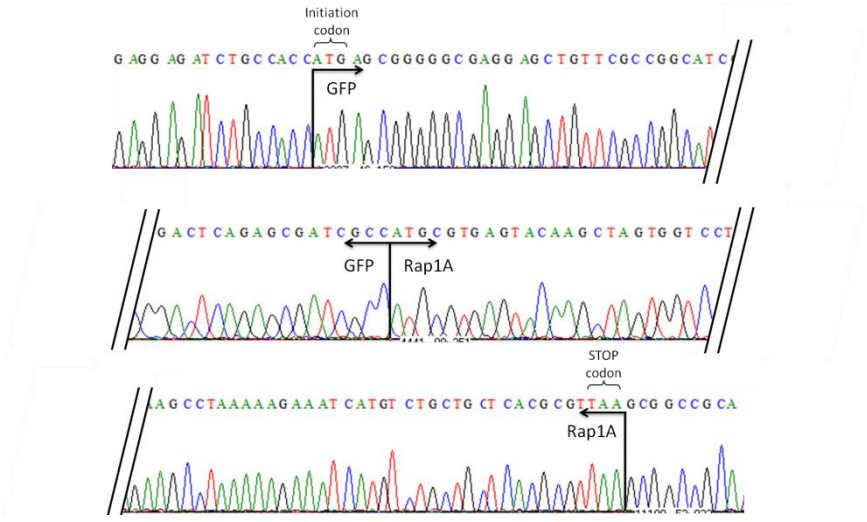

Figure 4.5 - Sequencing results for the ligation product pCMV6-AN-GFP-Rap1A (clone 6), showing correct insertion of the Rap1A cDNA directly downstream of the GFP cDNA and in frame.

After finishing the cloning, an additional mutagenesis reaction had to be performed. The Rap1A ORF from the original plasmid didn't have an endogenous STOP codon, as it was tagged with the GFP in the C-terminus, and the destination plasmid is built in such a way that it appends two codons to the end of the ORF before

the STOP codon in order to generate a suitable MluI restriction site in its C-terminus. Having two additional aminoacid residues in the C-terminus of the protein would likely prevent recognition of the prenylation site mentioned before, altering the protein's localization and function. Therefore, this mutagenesis was performed using the primers TAAins (see section 3.1.8), which were designed to insert a STOP codon (TAA) between the desired last codon of the ORF and the two unwanted, additional codons. The mutagenesis products were sequenced and the insertion of the STOP codon confirmed shown in Figure 4.6, with the plasmid being considered suitable for further use.

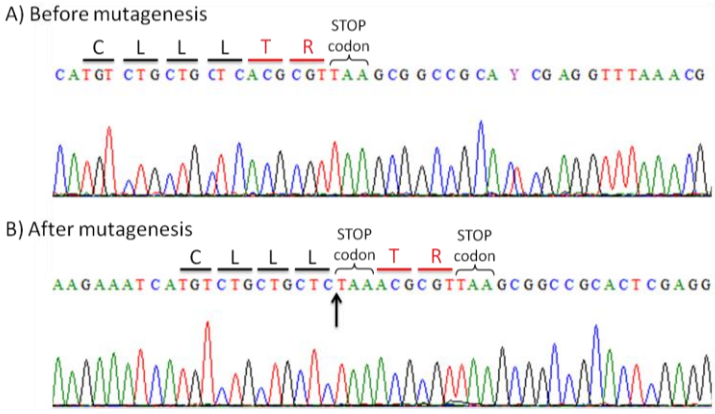

Figure 4.6 - Sequencing results confirming correct insertion of a STOP codon at the end of the Rap1A ORF. The two additional codons are highlighted in red.

Finally, the constitutively active and dominant negative mutants were produced, using the G12V, G15D and S17A primers and the programs described in section 3.1.8. Even after trying to optimize the PCR conditions, the mutagenesis for the G15D mutant was unsuccessful. All clones picked showed insertion of one or more sets of primers into the target region of the plasmid, possibly due to self complementarity of the primers. The production of this mutant was therefore abandoned due to time constraints. The products of the other two mutagenesis reactions were used to transform bacteria, purified and sequenced, as shown in Figure 4.7, confirming successful introduction of mutations and no further unwanted alterations.

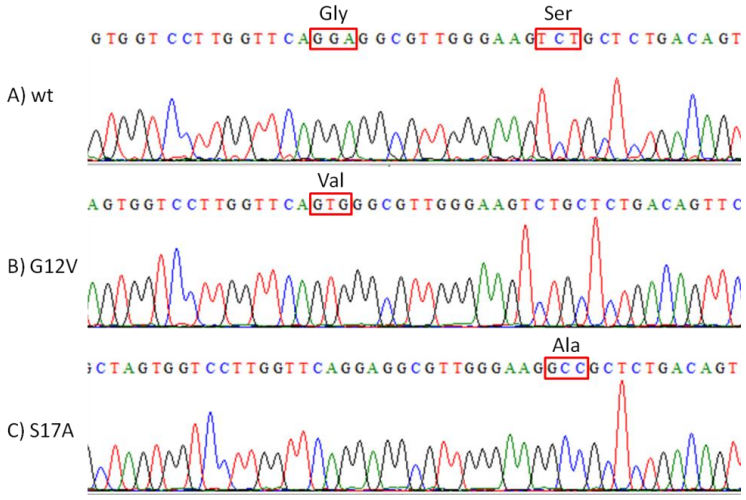

Figure 4.7 - Sequencing results confirming correct production of the constitutively active (G12V) and dominant negative (S17A) mutants.

4.4 Transfection optimization

Two transfection methods were used in the course of this work, electroporation and lipofection. The latter was performed with three different reagents, Lipofectamine 2000, Fugene HD and Hiperfect.

The CFBE cell line is an immortalized epithelial line that is not particularly easy to transfect, as occurs for epithelial cells in general. Initially, transfection with the empty pCMV6-AN-GFP vector, which only encodes for GFP, using Lipofectamine 2000 yielded very few transfected cells and low cell viability. High transfection efficiency is necessary to see any possible effect of Rap1A on CFTR biogenesis, particularly if this effect is of small magnitude; otherwise, changes in a few transfected cells won't be seen in experiments made with the whole cell population. Good cell viability is also important, particularly for CFTR function analysis in Ussing chambers, where a tight, polarized and completely confluent monolayer of cells is required. Thus, it became necessary to optimize the transfection procedure. The outcome of this optimization is summarized in Table 4.1.

Table 4.1 – Transfection efficiency and cell survival rate of the best conditions for each method used.

	DNA		siRNA	
Transfection Method	Efficiency	Survival rate	Knockdown efficiency	Survival rate
Electroporation	30-40%	10-20%	80-90%	75%
Lipofectamine 2000	10-20%	30-40%	20%	90-100%
Fugene HD	30-40%	90%	-	-
Hiperfect	-	-	55%	80-90%

For plasmid transfection, Lipofectamine 2000, Fugene HD and electroporation were used. In the beginning of the optimization process, transfection efficiency and cell viability were only monitored visually, as the plasmids encode for GFP or GFP constructs. When the need for more objective criteria was acknowledged, transfection efficiencies were estimated by directly counting green and total cells in the epifluorescence microscope in at least three different visual fields. This was only possible when cell viability was low and become unfeasible when many cells survived. A more accurate alternative would have been to trypsinize the cells before the experiment and count them in a haemocytometer.

Several experiments were made with Lipofectamine with varying Lipofectamine volumes and DNA amounts, but even the best conditions yielded very low transfection efficiency, about 10%, and very few cells survived. Electroporation yielded higher efficiencies of about 30-40%, depending on the plasmid, but few cells survived as well. Fugene HD was the selected method of choice for plasmids, as it yielded about 30-40% efficiencies and had a very high survival rate, with cells practically reaching confluence 48h later. For an illustrative Western Blot with extracts of cells transfected with FuGene, see Figure 4.9. This efficiency is still not as high as would be desirable, but it was as much as could be obtained.

It should be noted that transfection efficiency and fluorescence intensity in transfected cells were highly dependent on the plasmid. The plasmid encoding for the constitutively active mutant yielded the highest number of transfected cells and cells were brightly fluorescent. The dominant negative variant was the opposite, giving few and dimly fluorescent transfected cells, and the wt plasmid was in between. This was consistent between experiments and reagents.

For siRNA transfection, Lipofectamine 2000, Hiperfect and electroporation were used. Evaluating knockdown was only possible through Western Blot analysis. A validated siRNA against CFTR was used as a positive control and a scrambled siRNA was used as a negative control in order to discard non-specific effects. Lipofectamine was ineffective, having caused comparable decreases in CFTR levels with the scrambled and the CFTR-specific siRNA. Transfection of the CFTR siRNA with Hiperfect resulted in more pronounced decreases, having diminished CFTR levels to approximately 45% of the levels in non-transfected cells and Rap1A to approximately 20%, with viabilities between 80-90%. Electroporation, albeit being more aggressive to the cells and killing about 25% of them, was the most effective method by far, causing

a decrease in protein levels of up to 80-90%, and was thus considered the method of choice for siRNA transfection. These results (n=1) are illustrated in Figure 4.8.

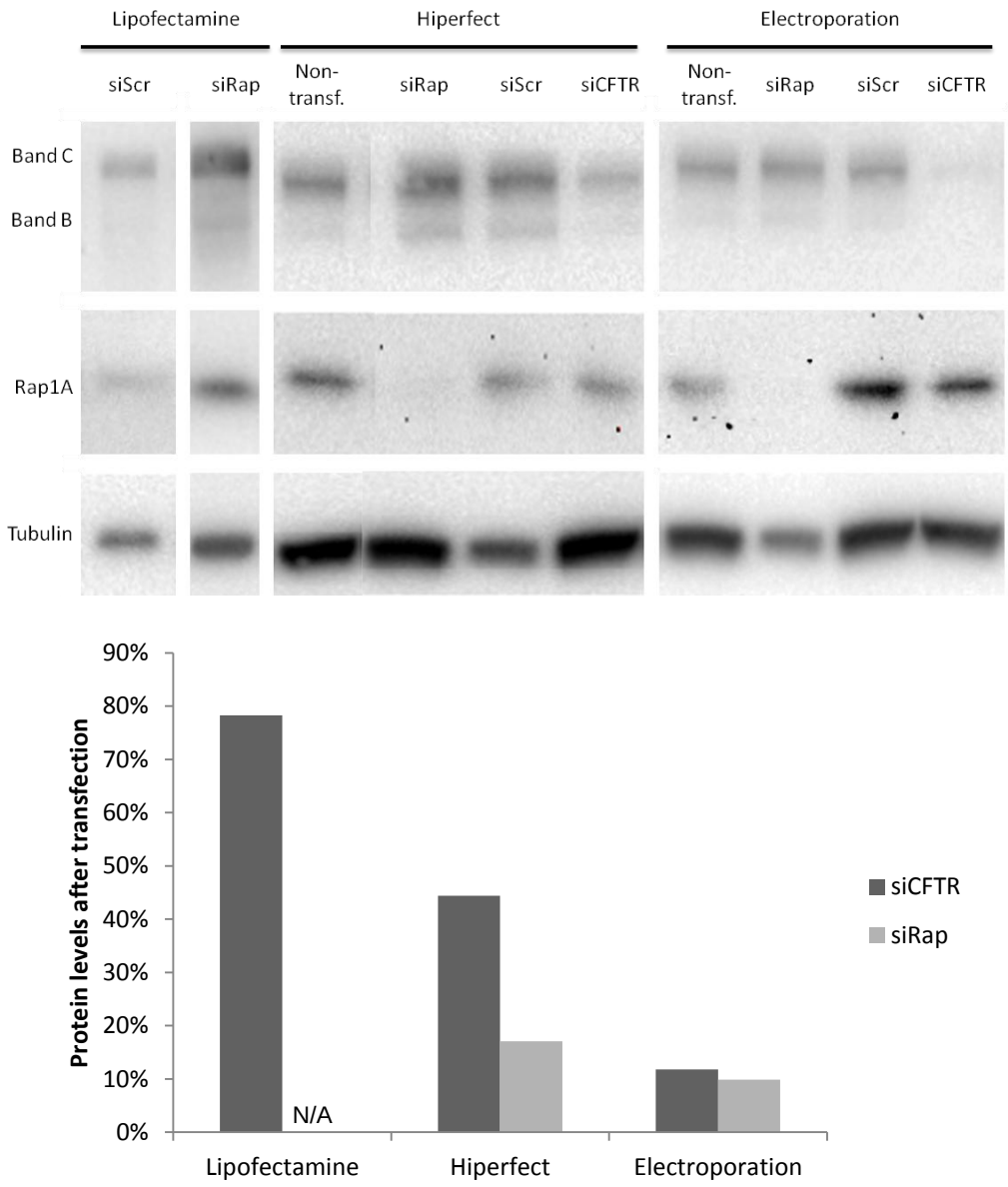

Figure 4.8- Comparison of knockdown efficiency with different transfection methods. Protein levels are expressed as percentage of the targeted protein in non-transfected samples; CFTR levels correspond to total CFTR (Band B + Band C). Rap1A levels after transfection with Lipofectamine were not available, due to problems with detection in the Western Blot. N=1.

In all of these transfection experiments, cells were seeded in uncoated plates. At a certain point, the question arose of whether the lack of coating was making it harder for the cells to adhere to the plates, as this might contribute to the high death rates that were being obtained so far. An experiment was made in which the cells were transfected with pCMV6-AN-GFP, pCMV6-AN-GFP-Rap1A or without DNA and seeded in parallel into coated and uncoated plates, but no difference in either cell survival or transfection efficiency was observed. A different protocol in which the cells were

already seeded and about 60-80% confluent at the time of transfection was also performed, but resulted in a much lower efficiency.

4.5 Rap1A expression and activity and its impact on steady-state CFTR

When suitable transfection conditions were defined, CFBE cells were transfected with the several plasmids available. The expression of Rap1A and CFTR was evaluated by Western Blotting. In parallel, a pull-down based Rap1A activity assay (described in section 3.2.5) was also performed, with two objectives: to confirm that the constitutively active and dominant negative mutants were behaving as expected and to see if the increase in total Rap1A protein was accompanied by an increase in active Rap1A. This last topic is important because signaling by small GTPases is regulated mainly by changes in their activation state, rather than by modulating the amount of the GTPase, as can be inferred by the large amount of different GEFs and GAPs existent. Results are shown in Figure 4.9.

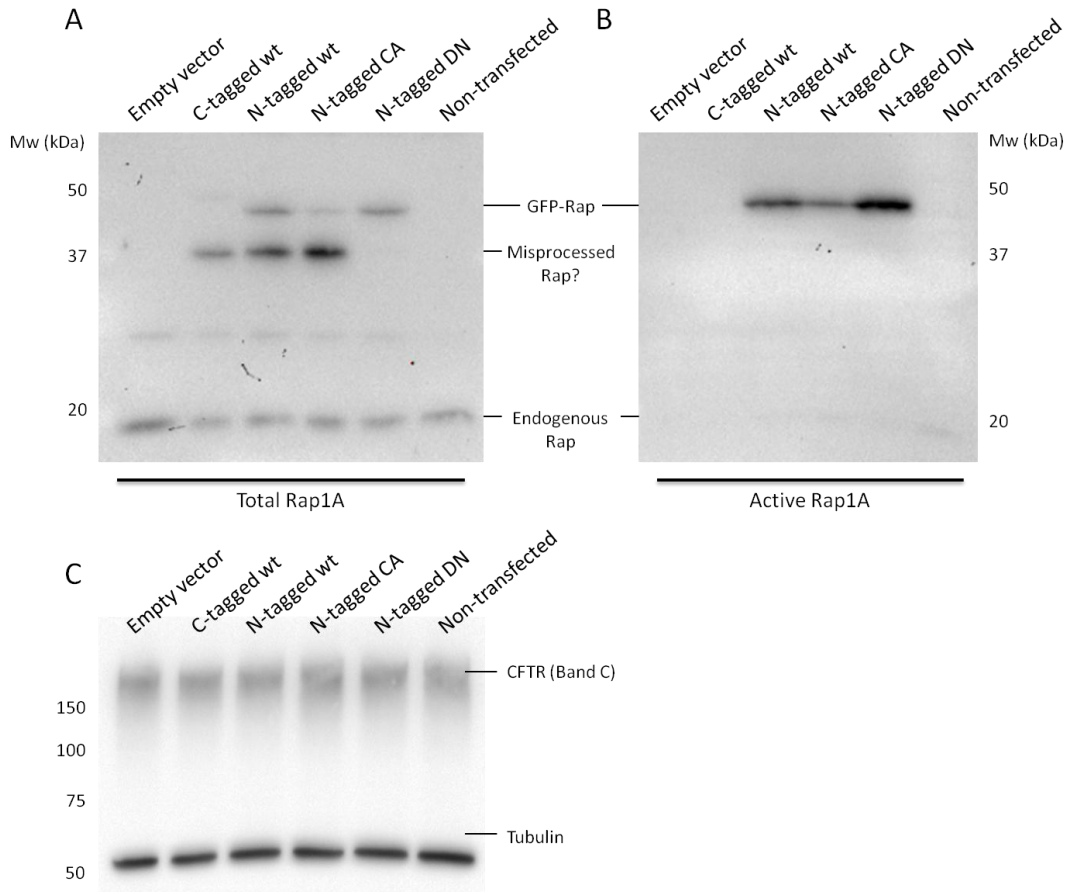

Figure 4.9 – Rap1A expression and activity and its effect in steady-state CFTR. Western Blots of Rap1A in (A) whole cell extracts and (B) active Rap1A precipitates of cells transfected with the several plasmid constructs available. (C) Western Blot of CFTR. Figures are representative of three experiments.

The C-tagged wt construct is not expressed with the expected molecular weight of ~47kDa. This is not surprising, as the CAAX motif, which is responsible for correct post-translational modification of the protein to its mature, membrane-bound form, is in the middle of the protein and not in the C-terminus as in the wt protein. Therefore, this construct is probably misprocessed; this would correspond to the band with smaller electrophoretic mobility that is present in the respective lane in the blot. This is compatible with the fact that there is no band in the active Rap1A blot for this construct.

Surprisingly, though, the N-tagged wt and constitutively active variants also show this band, and it is actually more intense than the one with the expected molecular mass. This probably means that, maybe due to the bulky GFP-tag, these constructs are not being correctly processed. The GFP tag might somehow sterically hinder the access of processing enzymes to the CAAX motif. Another possibility is that due to the GFP tag a fraction of the protein is locked in a conformation where that motif is masked, preventing the correct processing of the protein and its membrane targeting. Whatever the reason may be, this fraction of the protein does not show up in the active Rap1A blot, and is therefore not active. The correctly processed fractions of both constructs are active. The amount of active Rap1A seems to be proportional to the total amount of Rap1A, suggesting that the wt protein already displays high activation levels. These activation levels are probably intrinsic to the protein and not due to tonic activation by GEFs, because the endogenous protein barely showed up in the blots, so it should be mostly inactive.

Curiously, the dominant negative mutant doesn't show the lower molecular mass band. Furthermore, it gave an intense band in the active Rap1A blot, which can mean one of two things: either it is effectively active, or it is not active but still has affinity for the bait used in the Rap1A activity assay, in contradiction with the literature[66].

Taken together, these results motivated the exclusion of both G12V and S17A mutants from this study. Because the wt construct already shows high activation levels, the G12V mutant became obsolete. The S17A mutant, on the other hand, did not behave as a dominant negative at all, so it was discarded as well. The experiments continued with the wt construct only; despite of a good portion of it being assumedly misprocessed, a significant fraction still showed up at the expected molecular mass in the Western blots. The fact that it showed such intense bands in the active Rap1A blot is not ideal, but it should still allow for further work.

No significant alterations to the amount of steady-state CFTR were observed with any of the constructs. This might be because Rap1A has no effect on CFTR biogenesis at all in the conditions of these experiments or because the effect is too small to be

observed, due to the rather low transfection efficiency (30-40%) or to the small amount of functional exogenous Rap1A in transfected cells. These results might have been different if the cells were grown in filters and allowed to polarize; however, transfection of polarized CFBE cells is even more difficult to achieve, as can be seen later in section 4.6, especially with plasmid DNA.

4.6 Ussing chamber analysis of CFTR function upon down-regulation of Rap1A

CFBE cells overexpressing wt CFTR were transiently transfected in suspension with scrambled siRNA or Rap1A siRNA using Lipofectamine 2000 and seeded in coated Snapwell filters. Transepithelial resistance was measured 96h post-transfection and found to be between 750 and 1960 $\Omega.cm^2$, which indicates that the cell monolayer was electrically tight and polarized enough for Ussing chamber analysis.

The Ussing chamber protocol was then performed. Briefly, the cells were perfused in the luminal side with:

1) Ringer solution

2) Forskolin 2μM; forskolin is an adenylate cyclase agonist which rapidly increases cAMP levels in the cells; for this reason, it is used as a CFTR activator[63].

3) Forskolin 2μM + genistein 25μM; genistein is a CFTR potentiator and increases forskolin-induced chloride currents both in wt and F508del CFTR[67].

4) CFTR Inh172 30μM, a commonly used specific inhibitor of CFTR currents.[68]

Shown in Figure 4.10 are representative tracings of each experience.

Figure 4.10 - Ussing chamber measurement of CFTR funtion upon downregulation of Rap1A. Tracings are original recordings representative of 3 and 4 experiments with cells treated with siScrambled and siRap1A, respectively.

The results of the Ussing chamber experiments were then quantified and summarized in Figure **4.11**.

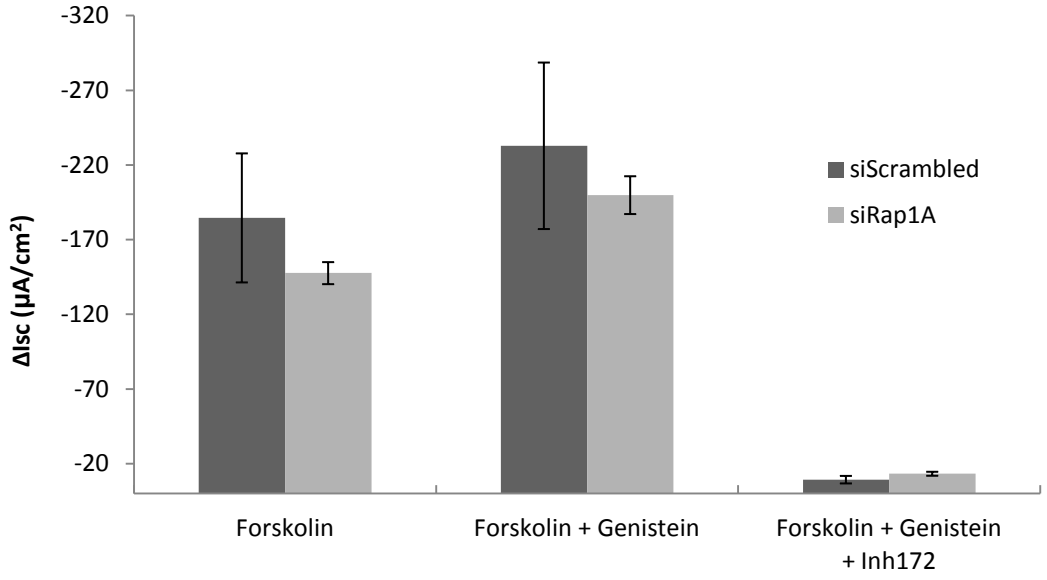

Figure 4.11 **- Effect of Rap1A down-regulation in CFTR function. CFBE cells were transiently transfected with siScrambled (n=4) or siRap1A (n=3) and polarized in Snapwell filters. 96h post-transfections, cell monolayers were perfused in Ussing chambers with Ringer solution (control), forskolin 2μM, forskolin 2μM + genistein 25μM and CFTR inh172 30μM. Transepithelial voltage and transepithelial resistance were measured and converted into equivalent short-circuit current measurements. Values are means + SEM.**

No statistically significant differences were measured between the currents elicited in siRap1A-transfected cells relative to siScrambled-transfected cells. After completion of the experiments, cells were lysed in 1x sample buffer and subjected to Western Blot for analysis of CFTR and Rap1A expression.

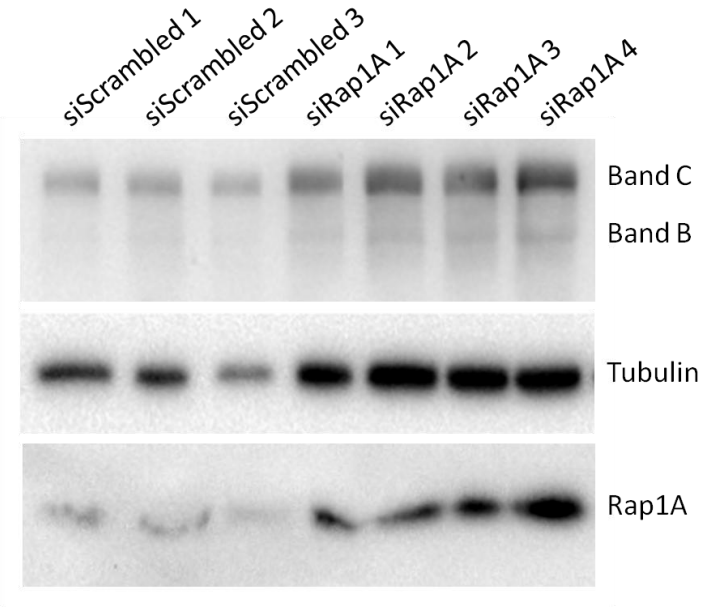

Figure 4.12 - Western Blot analysis of CFTR, tubulin and Rap1A expression in the cells used for the Ussing chamber experiment.

Because the lanes had different amounts of total protein, as assessed by the different intensities of the tubulin bands, band intensities needed to be quantified to allow for correct interpretation of the Western Blot. After normalizing CFTR and Rap1A band intensities to tubulin band intensities, there was no significant difference between Rap1A expression in cells transfected with siRap1A and siScrambled (p=0,40). This indicates that the transfection was not efficient; the consequence of this is that it is difficult to draw conclusive outcomes from the Ussing chamber functional assessment. If Rap1A down-regulation has some impact on CFTR expression and trafficking (as seen by Western Blot), as well as in its function (as seen by Ussing chamber analysis), this can only be seen if Rap1A is efficiently down-regulated, otherwise the effect is very small and becomes masked by the experimental noise.

The expression of Rap1A and CFTR was then analysed in each sample. Treating the data this way has the advantage that all the samples are treated equally instead of being grouped into two distinct classes which were not significantly different from one another in this experiment. Besides, Rap1A values in each class were not very homogeneous, probably due to differences in transfection efficiency and/or survival and growth rates in each sample; this too is disadvantageous when dealing with a class-based analysis.

The Band C/Band B ratios, indicative of the proportion of CFTR that has been correctly processed, and the forskolin-induced and genistein-induced I_{sc} values did not correlate well with Rap1A levels. However, there seems to be a tendency for higher

total CFTR expression and higher band C intensities in samples in which Rap1A is more expressed, as evidenced in Figure 4.13.

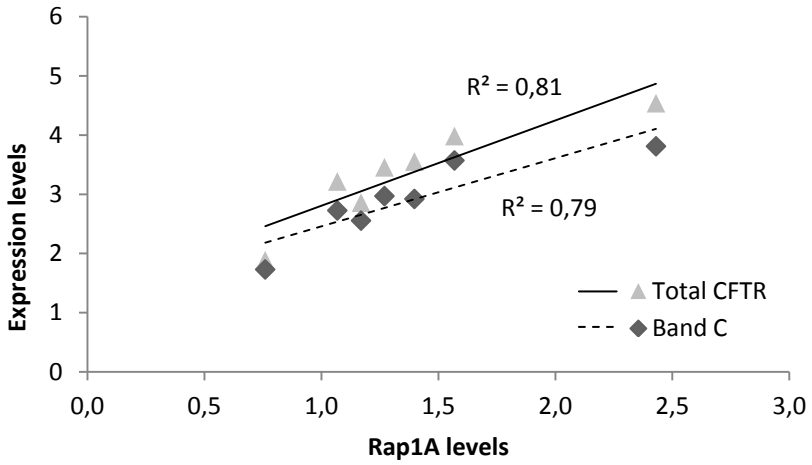

Figure 4.13 – Relationship between Rap1A and CFTR expression. Total CFTR levels refer to the cumulative intensities of band C and band B. Both CFTR and Rap1A band intensities were normalized to the respective tubulin band intensities. Linear regression was done using the least squares method.

5 Discussion

5.1 Validation of the central questions

As described in section 1.7, the two central questions this thesis tries to answer were prompted by results from former colleagues who performed a screen for potential CFTR-interacting proteins using an affinity purification protocol where proteins that interacted with the NBD1 of CFTR in Calu-3 cell extracts were captured. This was followed by separation of the captured proteins by 2D gel electrophoresis and their identification by mass spectrometry. One of the hits in this screen was identified as being the small GTPase Rap1A. However, further analysis of the mass spectrometry data revealed that this was probably a misidentification.

First of all, there was a discrepancy between the molecular weight of the spot in the gel (85kDa) and the associated hit obtained by analysis of the MS data with the Mascot software (21kDa). Furthermore, the hit was described in early, non-published reports as Raichu404X (Genbank ID BAB61868), not Rap1A. Raichu404X is an artificial construct that functions as an auto-FRET probe, and it is used to view Rap1A activation in the cell using fluorescence microscopy. It is thus not to be expected that such an artificial construct would be expressed in the Calu-3 cell line. Also, only one peptide fragment was used for this identification in the mass spectrometry study.

In light of this, there is no reason to believe Raichu404X was indeed the protein identified in the screen. A much more appealing candidate would have been phospholipase C β3, a more expectable hit that came with a lower score.

The possibility of the existence of a complex containing Rap1A and CFTR still exists, although to my knowledge there is no data in the literature that directly support this hypothesis. However, even if there is no physical interaction between Rap1A and CFTR, this GTPase may have an effect, albeit indirect, on CFTR biogenesis. Rap1 signaling has a known role in exocitosis in specialized cells, namely sperm[69], neurons and insulin secreting beta-cells[70,71]. Also, Rap1A is involved in E-cadherin recycling via vesicles containing Rab11 vesicles, and CFTR recycling also requires Rab11-positive vesicles. Since recycling of CFTR has an important role in the amount of protein at the plasma membrane[26], this is a process in which Rap1A could affect its steady-state membrane levels. Rap1A has also been shown to be necessary for proper polarization of neurons[72,73], yeasts[55], endothelial cells[53] and lymphocytes[74] and it seems to have some role in the establishment of polarity in epithelial cells[56,75]. This makes it likely that it will exert some kind of influence on CFTR, since trafficking of CFTR to the membrane is dependent on cell differentiation and polarization[76]. In addition to this, Rap1A is a known regulator of the Rho signaling pathway[48], which controls cytoskeletal dynamics and, specifically, CFTR stability in the plasma membrane via ezrin (Paulo Matos, personal communication). Finally, the RapGEF Epac can be located at the membrane by ezrin, and Epac-Radixin-PKA complexes[45], as well as ezrin-PKA-CFTR complexes[12] have been reported in the literature. This makes it possible that a Rap activator and Rap itself are very close to CFTR. Coincidentally, this GEF activates Rap in response to the same stimuli that activate CFTR.

All this data supports the hypothesis that Rap signaling has a potential effect on CFTR trafficking and function. Since Rap1A is expressed in primary cultures of human bronchial epitelial cells, as well as in the epitelial cell line used, as was seen by Western Blot in this work, it seems valid to question whether Rap1A affects CFTR biogenesis, trafficking and function.

5.2 Objective 1 – Producing plasmid constructs

The first objective consisted in producing plasmid constructs for expression of GFP-tagged wt, constitutively active and dominant negative Rap1A. These constructs were produced and they allowed for expression of these Rap1A variants; however, these constructs seem to express variants of the protein with disrupted folding and/or processing of the protein, which can be seen by the appearance of a band of higher

electrophoretic mobility in the Western Blots. This band was expected to appear in the C-tagged construct, due to masking of the –CAAX motif, but not in the other constructs. The presence of some misfolded or misprocessed recombinant protein wouldn't normally be too much of a problem, except that it was considerably more abundant than the correctly folded/processed protein for the wt and constitutively active constructs. Besides, accumulation of misfolded or misprocessed protein can trigger an unfolded protein response (UPS) in the cell[77], likely affecting CFTR biogenesis and confusing the results. The most plausible for this problem is the size of the GFP tag, which increases by approximately two-fold the size of the expressed protein when compared to Rap1A alone.

5.3 Objective 2 – Optimizing transfection and assessing Rap1A expression and activity

One of the major problems in this work was the fact that CFBE cells are hard to transfect, as it happens for epithelial cells in general[78]. Even with several attempts at optimizing the procedures and using several liposomal reagents, transfection of plasmid DNA yielded 30-40% efficiencies at best, which were not enough to detect an effect with statistical significance.

The results of the Rap1A activity assays were unexpected. The fact that the dominant negative S17A mutant gave intense bands in the activity assay is in direct contradiction with the literature[66]. It is possible that the GFP tag stabilizes the GTP bound conformation of Rap1A S17A, or that it facilitates an interaction between Rap1A and the RalGDS-RBD (the bait used in the assay) or even that GFP itself is capable of binding RalGDS-RBD.

It is important to note that the assay used is not exactly an activity assay in the common sense of the term, but rather a binding assay. Because Rap1A function is directly related to its ability of binding effectors and inducing conformational alterations in them, its affinity for the effectors is generally assumed to be a measure of its biological activity. Whether the S17A protein pulled-down was in fact active or was caused be artifactual binding of the protein to the bait remains to be seen. A way to test this hypothesis would be to measure an actual output of Rap1A activation, like B-Raf activation, in the cells transfected with the S17A construct versus cells transfected with non-tagged wt Rap1A.

The fact that the wt and constitutively active constructs yielded bands of relatively similar intensity might be due to tonic activation of Rap1A in these cells in the culture conditions used; however, active endogenous Rap1A levels seemed low compared to

exogenous active Rap1A levels, which makes this hypothesis unlikely. A more plausible explanation is that the G12V mutant is not entirely unsensitive to RapGAPs, even though it is established in the literature as a *bona fide* constitutively active mutant. In fact, Brinkmann and colleagues have shown that the G12V mutant is inactivated by RapGAP1[79]. An alternative mutant might be F64A, which is not inactivated by this GAP.

5.4 Objective 3 – Validating the CFTR-Rap1A interaction

Accounting for the increasing number of cellular processes, especially those related to cell differentiation and protein trafficking in which CFTR seems to play an active role, an interaction between CFTR and Rap1A is possible, especially if taking into account that interactions between Epac, ezrin/radixin, PKA and CFTR have been reported. The main strategy for validating this interaction was, as is usual in this kind of studies, immunoprecipitation. However, detecting Rap1A was very difficult. Optimization of Western blot for Rap1A achieved during the final stages of this work will allow these experiments to be performed, and thus to evaluate properly the interaction between CFTR and endogenous Rap1A. Testing this with overexpressed Rap1A should only be done when more appropriate constructs are generated, because not only is the bulky GFP tag likely to disrupt the folding and/or processing of Rap1A, it might also interfere with such an interaction.

5.5 Objective 4 – Effect of up and down-regulation of Rap1A on CFTR

The Ussing chamber experiments did not reveal any significant differences in CFTR function upon downregulation of Rap1A. This probably arises from the modest transfection efficiencies obtained, not necessarily from a lack of effect. It is also important to notice that there is the possibility that other Rap family members might compensate for the loss of Rap1A, since at least some of their functions are redundant. In fact, in many papers Rap1A and Rap1B are treated as a single entity, even though in fact they are two different proteins (which is somewhat misleading, though, because despite their 95% homology, their functions are not completely overlapping[38]). Besides, most research so far has focused on Rap1, leaving Rap2 proteins relatively obscure; they may also at least partially compensate for the loss of Rap1A.

It is usual in this kind of experiments to do a comparison with non-treated cell monolayers as a negative control. This would have allowed to see if the lack of difference in Rap levels between scrambled and Rap siRNA were due to the scrambled siRNA down-regulating Rap as an off-target effect. However, this didn't happen in other transfections, so it's an unlikely possibility. Besides, due to time constraints,

comparison of Rap siRNA with scrambled siRNA only was considered priority. For further experiments, electroporation would definitely be preferred, since it yielded a much better knockdown efficiency than using Lipofectamine.

It would be convenient to perform these experiments not only with downregulation of Rap1A using siRNAs, but also with overexpression using the plasmid constructs. Again, this should only be done when the appropriate constructs are generated, since the folding and/or processing of the GTPase seem to be disrupted, likely affecting its function. This would also require a more efficient transfection, relying in either a different protocol or a more manageable cell line.

6 Future perspectives

Although some of the objectives have not been achieved, this work allows the establishment of a more appropriate experimental layout. The main challenges to reaching the preset goals were the rather inefficient transfection protocols and the fact that the protein constructs didn't behave entirely as expected.

In further studies, there are at least two options to circumvent the transfection efficiency issue: either another protocol should be preferred (reverse transfection, for instance) or another cell line that is easier to transfect is used. An attractive candidate would be the A549 cell line, which is also a lung epithelial line. The main disadvantage over CFBE cells is that A549 cells don't polarize when grown in filters, therefore not being eligible for Ussing chamber experiments or to study cellular differentiation processes that depend on cellular polarization; alternatively, CFTR function could be studied using iodide efflux assays.

GFP-tagged small GTPases are not common in the literature. Even though it is a small protein, GFP is still bigger than Rap1A, so effects on Rap1A folding, processing and interactions with partners are not totally surprising. A smaller tag, like FLAG, on the N-terminus would be preferable[80]. This would require additional rounds of mutagenesis and cloning to be performed. Evaluating transfection efficiency would require Western Blotting, which is less practical than with a fluorescent tag; however, immunofluorescence and immunoprecipitation might be easier to do, as the antibodies directed against this kind of tags are usually quite good for either technique.

Additionally, several experiments remain to be performed. It would be interesting to evaluate the impact of Rap1A on CFTR stability at the membrane using modified pulse-chase approaches, as well as on its endocytosis and recycling rates using biotinylation protocols. It would also be interesting to use the Epac-selective cAMP analogue 8-pCPT-2'-O-Me-cAMP-AM to study how this RapGEF impacts CFTR function (Ussing chamber/iodide efflux) and maturation and amount in the membrane (Western Blot).

7 Bibliography

1. Francis S. Collins Cystic fibrosis: molecular biology and therapeutic implications. *Science* **256**, 774–779 (1992).
2. Riordan, J. R. *et al.* Identification of the cystic fibrosis gene: cloning and characterization of complementary DNA. *Science* **245**, 1066–1073 (1989).
3. Cystic Fibrosis Mutation Database: Statistics. at <http://www.genet.sickkids.on.ca/StatisticsPage.html>
4. Heijerman, H. Infection and inflammation in cystic fibrosis: A short review. *Journal of Cystic Fibrosis* **4, Supplement 2**, 3–5 (2005).
5. Steven Rowe, Stacey Miller & Eric Sorscher Cystic Fibrosis. *The New England Journal of Medicine* **352**, 1992–2001 (2005).
6. Amaral, M. D. & Kunzelmann, K. Molecular targeting of CFTR as a therapeutic approach to cystic fibrosis. *Trends in pharmacological sciences* **28**, 334–341 (2007).
7. Cystic Fibrosis Foundation - Drug Development Pipeline. at <http://www.cff.org/research/DrugDevelopmentPipeline/>
8. Hwang, T.-C. & Sheppard, D. N. Gating of the CFTR Cl− channel by ATP-driven nucleotide-binding domain dimerisation. *J Physiol* **587**, 2151–2161 (2009).
9. Li, C. & Naren, A. P. Macromolecular complexes of cystic fibrosis transmembrane conductance regulator and its interacting partners. *Pharmacology & Therapeutics* **108**, 208–223 (2005).
10. Sheppard, D. N. & Welsh, M. J. Structure and Function of the CFTR Chloride Channel. *Physiol Rev* **79**, S23–S45 (1999).
11. Favia, M. *et al.* Na+/H+ Exchanger Regulatory Factor 1 Overexpression-dependent Increase of Cytoskeleton Organization Is Fundamental in the Rescue of F508del Cystic Fibrosis Transmembrane Conductance Regulator in Human Airway CFBE41o- Cells. *Mol. Biol. Cell* **21**, 73–86 (2010).
12. Sun, F. *et al.* E3KARP Mediates the Association of Ezrin and Protein Kinase A with the Cystic Fibrosis Transmembrane Conductance Regulator in Airway Cells. *J. Biol. Chem.* **275**, 29539–29546 (2000).
13. Hug, M. J., Tamada, T. & Bridges, R. J. CFTR and Bicarbonate Secretion to Epithelial Cells. *Physiology* **18**, 38–42 (2003).
14. Kim, D., Steward, M. C. & others The role of CFTR in bicarbonate secretion by pancreatic duct and airway epithelia. *J Med Invest* **56**, 336–342 (2009).
15. Hudson, V. M. Rethinking cystic fibrosis pathology: the critical role of abnormal reduced glutathione (GSH) transport caused by CFTR mutation. *Free Radical Biology and Medicine* **30**, 1440–1461 (2001).
16. Kogan, I. *et al.* CFTR directly mediates nucleotide-regulated glutathione flux. *EMBO J* **22**, 1981–1989 (2003).
17. Kunzelmann, K. & Schreiber, R. CFTR, a regulator of channels. *Journal of Membrane Biology* **168**, 1–8 (1999).
18. Kunzelmann, K. *et al.* The cystic fibrosis transmembrane conductance regulator attenuates the endogenous Ca^{2+} activated Cl^-; conductance of *Xenopus* oocytes. *Pflügers Archiv European Journal of Physiology* **435**, 178–181 (1997).
19. Lukacs, G. L. & Verkman, A. S. CFTR: folding, misfolding and correcting the ΔF508 conformational defect. *Trends in Molecular Medicine* **18**, 81–91 (2012).
20. Glozman, R. *et al.* N-glycans are direct determinants of CFTR folding and stability in secretory and endocytic membrane traffic. *J Cell Biol* **184**, 847–862 (2009).
21. Farinha, C. M. & Amaral, M. D. Most F508del-CFTR Is Targeted to Degradation at an Early Folding Checkpoint and Independently of Calnexin. *Mol Cell Biol* **25**, 5242–5252 (2005).
22. Amaral, M. D. Processing of CFTR: Traversing the cellular maze—How much CFTR needs to go through to avoid cystic fibrosis? *Pediatric pulmonology* **39**, 479–491 (2005).

23. Gee, H. Y., Noh, S. H., Tang, B. L., Kim, K. H. & Lee, M. G. Rescue of ΔF508-CFTR Trafficking via a GRASP-Dependent Unconventional Secretion Pathway. *Cell* **146**, 746–760 (2011).
24. Morris, A. P., Cunningham, S. A., Tousson, A., Benos, D. J. & Frizzell, R. A. Polarization-dependent apical membrane CFTR targeting underlies cAMP-stimulated Cl^- secretion in epithelial cells. *American Journal of Physiology-Cell Physiology* **266**, C254–C268 (1994).
25. Brown, D., Stow, J. Protein trafficking and polarity in kidney epithelium: from cell biology to physiology. *Physiological Reviews* **76**, (1996).
26. Ameen, N., Silvis, M. & Bradbury, N. A. Endocytic trafficking of CFTR in health and disease. *Journal of Cystic Fibrosis* **6**, 1–14 (2007).
27. Bertrand, C. A. & Frizzell, R. A. The role of regulated CFTR trafficking in epithelial secretion. *Am J Physiol Cell Physiol* **285**, C1–C18 (2003).
28. Henderson, M. J., Singh, O. V. & Zeitlin, P. L. Applications of proteomic technologies for understanding the premature proteolysis of CFTR. *Expert Rev Proteomics* **7**, 473–486 (2010).
29. Collawn, J. F., Fu, L. & Bebok, Z. Targets for cystic fibrosis therapy: proteomic analysis and correction of mutant cystic fibrosis transmembrane conductance regulator. *Expert Rev Proteomics* **7**, 495–506 (2010).
30. Faria, D. *et al.* Effect of Annexin A5 on CFTR: regulated traffic or scaffolding? *Molecular Membrane Biology* **28**, 14–29 (2011).
31. Bos, J. L. Linking Rap to cell adhesion. *Current Opinion in Cell Biology* **17**, 123–128 (2005).
32. Colicelli, J. Human RAS Superfamily Proteins and Related GTPases. *Sci. STKE* **2004**, re13 (2004).
33. Bokoch, G. M. Biology of the Rap proteins, members of the ras superfamily of GTP-binding proteins.pdf. *Biochem. J.* 17–24 (1993).
34. Hu, C. D. *et al.* Effect of phosphorylation on activities of Rap1A to interact with Raf-1 and to suppress Ras-dependent Raf-1 activation. *Journal of Biological Chemistry* **274**, 48–51 (1999).
35. Nomura, K., Kanemura, H., Satoh, T. & Kataoka, T. Identification of a Novel Domain of Ras and Rap1 That Directs Their Differential Subcellular Localizations. *J. Biol. Chem.* **279**, 22664–22673 (2004).
36. Pizon, V., Desjardins, M., Bucci, C., Parton, R. G. & Zerial, M. Association of Rap1a and Rap1b proteins with late endocytic/phagocytic compartments and Rap2a with the Golgi complex. *Journal of cell science* **107**, 1661–1670 (1994).
37. Pizon, V., Méchali, F. & Baldacci, G. RAP1A GTP/GDP Cycles Determine the Intracellular Location of the Late Endocytic Compartments and Contribute to Myogenic Differentiation. *Experimental Cell Research* **246**, 56–68 (1999).
38. Wittchen, E. S., Aghajanian, A. & Burridge, K. Isoform-specific differences between Rap1A and Rap1B GTPases in the formation of endothelial cell junctions. *Small GTPases* **2**, 65–76 (2011).
39. Jeong, H.-W., Li, Z., Brown, M. D. & Sacks, D. B. IQGAP1 Binds Rap1 and Modulates Its Activity. *Journal of Biological Chemistry* **282**, 20752–20762 (2007).
40. Asuri, S., Yan, J., Paranavitana, N. C. & Quilliam, L. A. E-cadherin dis-engagement activates the Rap1 GTPase. *J Cell Biochem* **105**, 1027–1037 (2008).
41. Béranger, F., Goud, B., Tavitian, A. & de Gunzburg, J. Association of the Ras-antagonistic Rap1/Krev-1 proteins with the Golgi complex. *Proc Natl Acad Sci U S A* **88**, 1606–1610 (1991).
42. Ross, S. H. *et al.* Ezrin is required for efficient Rap1-induced cell spreading. *Journal of Cell Science* **124**, 1808–1818 (2011).
43. Raaijmakers, J. H. & Bos, J. L. Specificity in Ras and Rap Signaling. *Journal of Biological Chemistry* **284**, 10995–10999 (2008).
44. Gloerich, M. & Bos, J. L. Regulating Rap small G-proteins in time and space. *Trends in Cell Biology* **21**, 615–623 (2011).

45. Hochbaum, D., Barila, G., Ribeiro-Neto, F. & Altschuler, D. L. Radixin Assembles cAMP Effectors Epac and PKA into a Functional cAMP Compartment: ROLE IN cAMP-DEPENDENT CELL PROLIFERATION. *Journal of Biological Chemistry* **286**, 859–866 (2010).
46. Kupzig, S., Bouyoucef-Cherchalli, D., Yarwood, S., Sessions, R. & Cullen, P. J. The Ability of GAP1IP4BP To Function as a Rap1 GTPase-Activating Protein (GAP) Requires Its Ras GAP-Related Domain and an Arginine Finger Rather than an Asparagine Thumb. *Mol. Cell. Biol.* **29**, 3929–3940 (2009).
47. Lafuente, E. M. *et al.* RIAM, an Ena/VASP and Profilin Ligand, Interacts with Rap1-GTP and Mediates Rap1-Induced Adhesion. *Developmental Cell* **7**, 585–595 (2004).
48. Arthur, W. T., Quilliam, L. A. & Cooper, J. A. Rap1 promotes cell spreading by localizing Rac guanine nucleotide exchange factors. *The Journal of cell biology* **167**, 111–122 (2004).
49. Fukuyama, T. *et al.* Involvement of the c-Src-Crk-C3G-Rap1 Signaling in the Nectin-induced Activation of Cdc42 and Formation of Adherens Junctions. *J. Biol. Chem.* **280**, 815–825 (2005).
50. Jeon, C.-Y. *et al.* p190RhoGAP and Rap-dependent RhoGAP (ARAP3) inactivate RhoA in response to nerve growth factor leading to neurite outgrowth from PC12 cells. *Exp Mol Med* **42**, 335–344 (2010).
51. Yamada, T., Sakisaka, T., Hisata, S., Baba, T. & Takai, Y. RA-RhoGAP, Rap-activated Rho GTPase-activating Protein Implicated in Neurite Outgrowth through Rho. *J. Biol. Chem.* **280**, 33026–33034 (2005).
52. Hoshino, T. *et al.* Regulation of E-cadherin Endocytosis by Nectin through Afadin, Rap1, and p120ctn. *J. Biol. Chem.* **280**, 24095–24103 (2005).
53. Lampugnani, M. G. *et al.* CCM1 Regulates Vascular-Lumen Organization by Inducing Endothelial Polarity. *J Cell Sci* **123**, 1073–1080 (2010).
54. Fu, D., Lippincott-Schwartz, J. & Arias, I. M. Cellular mechanism of bile acid-accelerated hepatocyte polarity. *Small Gtpases* **2**, 314–317 (2011).
55. Michelitch, M. & Chant, J. A mechanism of Bud1p GTPase action suggested by mutational analysis and immunolocalization. *Current Biology* **6**, 446–454 (1996).
56. Li, R. & Pendergast, A. M. Arg Kinase Regulates Epithelial Cell Polarity by Targeting β1-Integrin and Small GTPase Pathways. *Current Biology* **21**, 1534–1542 (2011).
57. Ehrhardt, C. *et al.* Towards an in vitro model of cystic fibrosis small airway epithelium: characterisation of the human bronchial epithelial cell line CFBE41o-. *Cell and Tissue Research* **323**, 405–415 (2006).
58. Fulcher, M., Gabriel, S., Burns, K., Yankaskas, J. & Randell, S. Methods in Molecular Medicine, vol. 107: Human Cell Culture Protocols.
59. Felgner, P. L. *et al.* Lipofection: a highly efficient, lipid-mediated DNA-transfection procedure. *PNAS* **84**, 7413–7417 (1987).
60. Gehl, J. Electroporation: theory and methods, perspectives for drug delivery, gene therapy and research. *Acta Physiologica Scandinavica* **177**, 437–447 (2003).
61. Franke, B., Akkerman, J. W. N. & Bos, J. L. Rapid Ca^{2+}-mediated activation of Rap1 in human platelets. *The EMBO journal* **16**, 252–259 (1997).
62. Li, H., Sheppard, D. N. & Hug, M. J. Transepithelial electrical measurements with the Ussing chamber. *Journal of Cystic Fibrosis* **3, Supplement 2**, 123–126 (2004).
63. Mall, M., Hirtz, S., Gonska, T. & Kunzelmann, K. Assessment of CFTR function in rectal biopsies for the diagnosis of cystic fibrosis. *Journal of Cystic Fibrosis* **3, Supplement 2**, 165–169 (2004).
64. Price, L. S. Rap1 Regulates E-cadherin-mediated Cell-Cell Adhesion. *Journal of Biological Chemistry* **279**, 35127–35132 (2004).
65. Liu, J. J. *et al.* A mechanism of Rap1-induced stabilization of endothelial cell–cell junctions. *Molecular biology of the cell* **22**, 2509–2519 (2011).

66. Dupuy, A. G. *et al.* Novel Rap1 dominant-negative mutants interfere selectively with C3G and Epac. *Oncogene* **24**, 4509–4520 (2005).
67. Hwang, T. C., Wang, F., Yang, I. C. & Reenstra, W. W. Genistein potentiates wild-type and ΔF508-CFTR channel activity. *Am. J. Physiol.* **273**, C988–998 (1997).
68. Caci, E. *et al.* Evidence for direct CFTR inhibition by CFTR(inh)-172 based on Arg347 mutagenesis. *Biochem. J.* **413**, 135–142 (2008).
69. Branham, M. T. *et al.* Epac Activates the Small G Proteins Rap1 and Rab3A to Achieve Exocytosis. *Journal of Biological Chemistry* **284**, 24825–24839 (2009).
70. Chepurny, O. G. *et al.* Enhanced Rap1 Activation and Insulin Secretagogue Properties of an Acetoxymethyl Ester of an Epac-selective Cyclic AMP Analog in Rat INS-1 Cells: STUDIES WITH 8-pCPT-2'-O-Me-cAMP-AM. *J. Biol. Chem.* **284**, 10728–10736 (2009).
71. Leech, C. A., Chepurny, O. G. & Holz, G. G. Epac2-Dependent Rap1 Activation and the Control of Islet Insulin Secretion by Glucagon-Like Peptide-1. *Vitam Horm* **84**, 279–302 (2010).
72. Jossin, Y. Polarization of migrating cortical neurons by Rap1 and N-cadherin. *Small Gtpases* **2**, 322–328 (2011).
73. Schwamborn, J. C., Müller, M., Becker, A. H. M. & Püschel, A. W. Ubiquitination of the GTPase Rap1B by the ubiquitin ligase Smurf2 is required for the establishment of neuronal polarity. *The EMBO journal* **26**, 1410–1422 (2007).
74. Freeman, S. A. *et al.* Preventing the Activation or Cycling of the Rap1 GTPase Alters Adhesion and Cytoskeletal Dynamics and Blocks Metastatic Melanoma Cell Extravasation into the Lungs. *Cancer Res* **70**, 4590–4601 (2010).
75. Itoh, M., Nelson, C. M., Myers, C. A. & Bissell, M. J. Rap1 integrates tissue polarity, lumen formation, and tumorigenic potential in human breast epithelial cells. *Cancer research* **67**, 4759 (2007).
76. Bebök, Z., Tousson, A., Schwiebert, L. M. & Venglarik, C. J. Improved oxygenation promotes CFTR maturation and trafficking in MDCK monolayers. *American Journal of Physiology-Cell Physiology* **280**, C135–C145 (2001).
77. Vabulas, R. M., Raychaudhuri, S., Hayer-Hartl, M. & Hartl, F. U. Protein Folding in the Cytoplasm and the Heat Shock Response. *Cold Spring Harb Perspect Biol* **2**, (2010).
78. Matsui, H., Johnson, L. G., Randell, S. H. & Boucher, R. C. Loss of Binding and Entry of Liposome-DNA Complexes Decreases Transfection Efficiency in Differentiated Airway Epithelial Cells. *J. Biol. Chem.* **272**, 1117–1126 (1997).
79. Brinkmann, T. *et al.* Rap-specific GTPase Activating Protein follows an Alternative Mechanism. *J. Biol. Chem.* **277**, 12525–12531 (2002).
80. Terpe, K. Overview of tag protein fusions: from molecular and biochemical fundamentals to commercial systems. *Applied microbiology and biotechnology* **60**, 523–533 (2003).

8 Appendices

8.1 Appendix I – pCMV6-AC-Rap1A-GFP plasmid map and cloning scheme

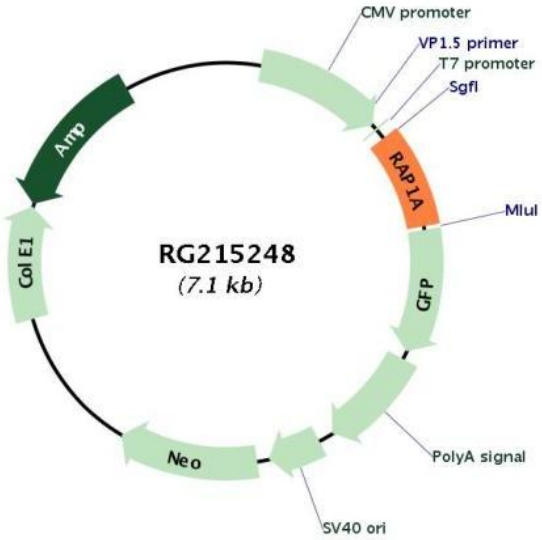

RBS Kozac Consensus

EcoRI BamHI KpnI BglII SgfI

```
ATAGGGCGGCCGGGAATTCGTCGACTGGATCCGGTACCGAGGAGATCTGCCGCCGCGATCGCC ATG CGT GAG TAC
                                                                  M   R   E   Y

AAG CTA GTG GTC CTT GGT TCA GGA GGC GTT GGG AAG TCT GCT CTG ACA GTT CAG TTT GTT
 K   L   V   V   L   G   S   G   G   V   G   K   S   A   L   T   V   Q   F   V

CAG GGA ATT TTT GTT GAA AAA TAT GAC CCA ACG ATA GAA GAT TCC TAC AGA AAG CAA GTT
 Q   G   I   F   V   E   K   Y   D   P   T   I   E   D   S   Y   R   K   Q   V

GAA GTC GAT TGC CAA CAG TGT ATG CTC GAA ATC CTG GAT ACT GCA GGG ACA GAG CAA TTT
 E   V   D   C   Q   Q   C   M   L   E   I   L   D   T   A   G   T   E   Q   F

ACA GCA ATG AGG GAT TTG TAT ATG AAG AAC GGC CAA GGT TTT GCA CTA GTA TAT TCT ATT
 T   A   M   R   D   L   Y   M   K   N   G   Q   G   F   A   L   V   Y   S   I

ACA GCT CAG TCC ACG TTT AAC GAC TTA CAG GAC CTG AGG GAA CAG ATT TTA CGG GTT AAG
 T   A   Q   S   T   F   N   D   L   Q   D   L   R   E   Q   I   L   R   V   K

GAC ACG GAA GAT GTT CCA ATG ATT TTG GTT GGC AAT AAA TGT GAC CTG GAA GAT GAG CGA
 D   T   E   D   V   P   M   I   L   V   G   N   K   C   D   L   E   D   E   R

GTA GTT GGC AAA GAG CAG GGC CAG AAT TTA GCA AGA CAG TGG TGT AAC TGT GCC TTT TTA
 V   V   G   K   E   Q   G   Q   N   L   A   R   Q   W   C   N   C   A   F   L

GAA TCT TCT GCA AAG TCA AAG ATC AAT GTT AAT GAG ATA TTT TAT GAC CTG GTC AGA CAG
 E   S   S   A   K   S   K   I   N   V   N   E   I   F   Y   D   L   V   R   Q

ATA AAT AGG AAA ACA CCA GTG GAA AAG AAG AAG CCT AAA AAG AAA TCA TGT CTG CTG CTC
 I   N   R   K   T   P   V   E   K   K   K   P   K   K   K   S   C   L   L   L

MluI   NotI   XhoI      GFP-tag                                PmeI   FseI   SacII
ACG CGT ACG CGG CCG CTC GAG ATG GAG AGC GAC ... GAA GAA AGA GTT TAA ACGGCCGGCCGC
 T   R   T   R   P   L   E   M   E   S   D   .   E   E   R   V   *

GGTC
```

8.2 Appendix II – pCMV6-AN-GFP plasmid map and cloning scheme

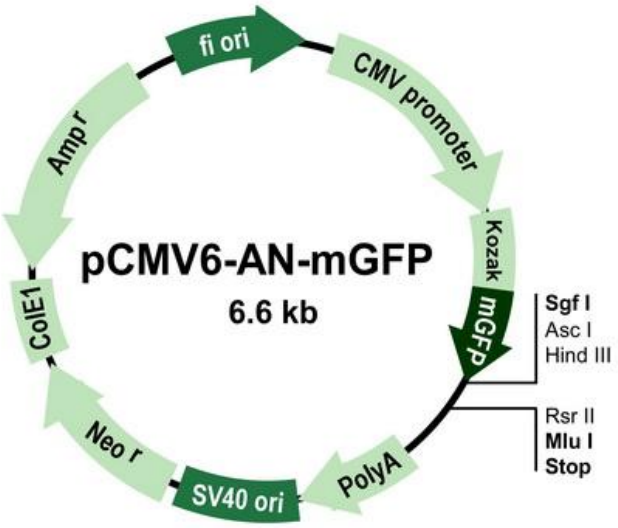

pCMV6-AN-mGFP

EcoR I BamH I Kpn I RBS Kozac Consensus mGFP Tag

CTATAGGGCGGCCGGGAATTCGTCGACTGGATCCGGTACCGAGGAGATCTGCCACC ATG AGC GGG GGC --- ---

M S G G - -

Sgf I Asc I Hind III Rsr II Mlu I

--- --- GGA CTC AGA GCG ATC GCCGGCGCGCCAGATCTCAAGCTTAACTAGTTAGCGGACCG ACG CGT TAA

- - G L R T R Stop

Not I Xho I Pme I Fse I

GCGGCCGCACTCGAGGTTTAAACGGCCGGCCGCGG

8.3 Appendix III – Preparation of GST-RalGDS-RBD-coupled beads for Rap1A activity assays

The GST-RalGDS-RBD-coupled beads had to be produced for the Rap1A activity assays. Bacteria transformed with the pGEX-GST-RalGDS-RBD were available from the start of the work. Recombinant protein expression had previously been shown to be maximal after 4 hours of incubation with IPTG.

To confirm expression of the recombinant protein, aliquots of bacteria were taken immediately before and 4h after incubation with IPTG, centrifuged at 4000g for 10min and lysed in 1x sample buffer. Extracts were run on an SDS-PAGE gel, which was then stained with Coomassie Blue, as can be seen in Figure 8.1.

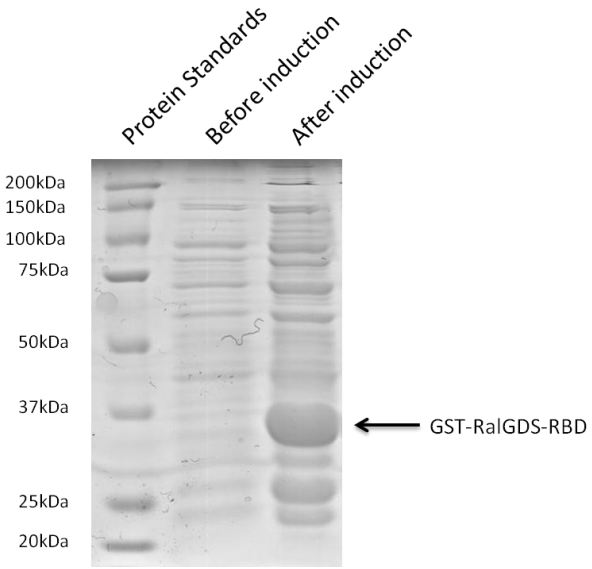

Figure 8.1 - Coomassie-stained SDS-PAGE gel showing expression of recombinant protein after induction with IPTG.

Recombinant protein expression was confirmed with the appearance of a strong band below the 37kDa marker.

To prepare the beads, it was still necessary to know how much glutathione-coupled agarose beads should be added to the bacterial extracts, which required knowing the amount of recombinant protein recovered. For this, increasing amounts of BSA were run on an SDS-PAGE gel, as well as an aliquot of the extract. The gel was then stained with Coomassie Blue and digitalized (Figure 8.2).

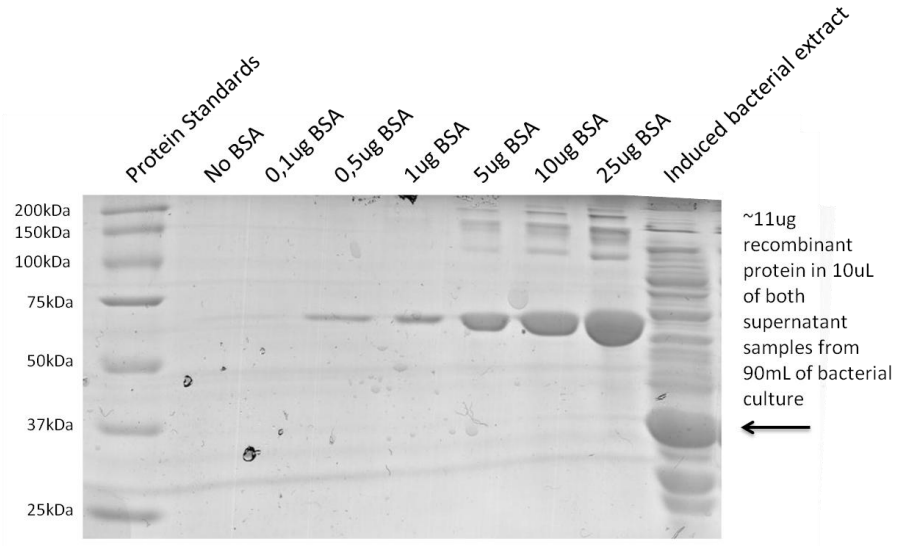

Figure 8.2 - SDS-PAGE gel for quantification of expressed GST-RalGDS-RBD.

BSA band intensities were then quantified and used to make a standard curve, which is represented in Figure 8.3.

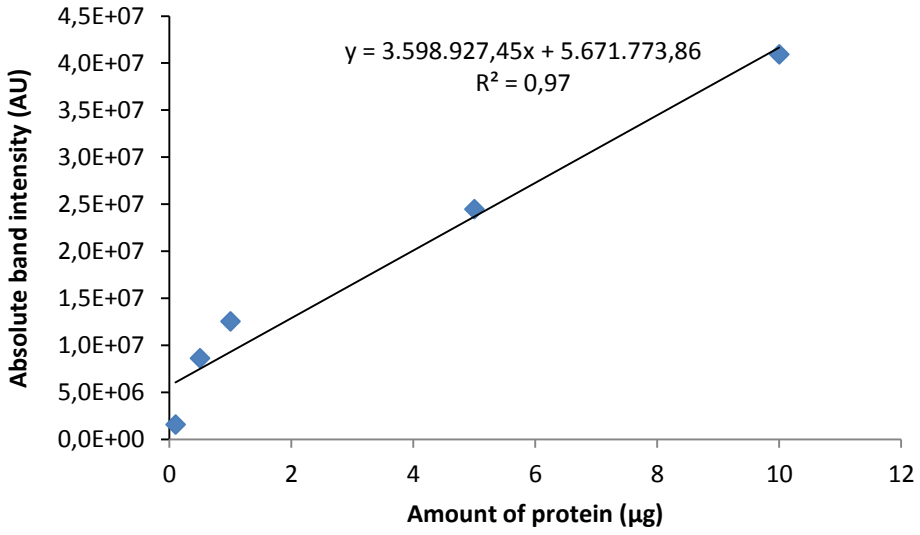

Figure 8.3 – BSA standard curve for the SDS-PAGE gel used for quantification of recombinant GST-RalGDS-RBD.

Finally, this standard curve was used to extrapolate the amount of protein in the bacterial extracts based on the respective band intensity on the gel, yielding a value of 1.82mg of recombinant protein. Since the manufacturer of the beads recommends 1mL of slurry for each 5-6mg of protein, 360uL of slurry was added to the extracts, which were then washed and stored as described in section 3.2.5.